



# RESEARCH MEMORANDUM

ANALYSIS OF EFFECTS OF AIRPLANE CHARACTERISTICS AND  
AUTOPILOT PARAMETERS ON A ROLL-COMMAND SYSTEM  
WITH AILERON RATE AND DEFLECTION LIMITING

By Albert A. Schy and Ordway B. Gates, Jr.

Langley Aeronautical Laboratory  
Langley Field, Va.

LIBRARY COPY

JUL 25 1955

LANGLEY RESEARCH CENTER  
LIBRARY, NASA

**NATIONAL ADVISORY COMMITTEE  
FOR AERONAUTICS**  
WASHINGTON

September 2, 1955  
Declassified September 9, 1958

NATIONAL ADVISORY COMMITTEE FOR AERONAUTICS

---

RESEARCH MEMORANDUM

---

ANALYSIS OF EFFECTS OF AIRPLANE CHARACTERISTICS AND  
AUTOPILOT PARAMETERS ON A ROLL-COMMAND SYSTEM  
WITH AILERON RATE AND DEFLECTION LIMITING

By Albert A. Schy and Ordway B. Gates, Jr.

SUMMARY

The dynamic characteristics of an airplane with a proportional-gain roll-control autopilot are discussed. The significant aspects of the dynamic characteristics of the airplane are analyzed. A comparison of three different high-speed fighter airplanes is presented. The dynamic effects of time lags and various gains in the system are described. Results obtained by the Reeves Electronic Analog Computer are presented to show the effects of limiting the aileron deflection and rate of deflection on the dynamic characteristics of the system.

INTRODUCTION

There is much interest at the present time in the development of a completely automatic interceptor system. Much research, both analytical and experimental, is being done toward the development of specific systems. However, there remains a serious lack of published material on many problems which would be of general interest to people in this field. For this reason, the Langley stability analysis section has undertaken an analog-simulation study of certain aspects of the attack phase of the automatic interception problem by using accurate simulation of airplane dynamics, attack geometry, and guidance computers.

In connection with this study, for which a large analog computer is needed, several investigations of particular aspects of the complete problem using appropriate approximations for simplified simulation are being carried out. Various simplifying approximations are often feasible when it is desired to investigate certain aspects of the attack problem individually. One purpose of these small-scale studies is to determine desirable characteristics for the tie-in equipment and autopilots for use in the large-scale analog simulation mentioned above.

A roll-command autopilot is an important component of any automatically controlled interceptor, because an airplane must bank in order to turn its flight path effectively. This paper presents the results of a theoretical investigation of a so-called proportional-gain roll-command autopilot. In this type of autopilot, the signal to the aileron servo consists essentially of a linear combination of the error in bank, its time derivatives and/or integrals, and various components of the airplane motion. The proportional amount of any component which enters into the aileron-actuating signal depends on the gain on this component.

By use of standard methods for the analysis of linear dynamic systems (see ref. 1, for example), the following aspects of the automatic roll-command system were investigated: the properties of the airplane as a component of the system, the effects of the various gains on the dynamic characteristics of the system, and the effects of time lags in the system. Also, the nonlinear effects of limiting the amplitude and rate of the aileron motion were investigated by use of a Reeves Electronic Analog Computer (REAC).

In order to investigate the effects of different airplane characteristics on the system, results were obtained for the following four cases: a present-day interceptor which has very little coupling between the rolling and yaw-sideslip motions; two flight conditions of a high-speed research airplane having relatively low roll inertia and damping, low Dutch-roll damping, and very high ratio of roll-to-sideslip magnitude in the Dutch-roll mode; and an advanced-design interceptor having good Dutch-roll damping due to a high stabilizing value of the product of inertia.

## SYMBOLS

$a_0, \dots, a_3$	coefficients of numerator of roll transfer function (see eq. (8))
$A_0, \dots, A_4$	coefficients of denominator of roll transfer function (see eq. (8))
arg	phase angle (argument) of a complex number, deg or radians
b	span, ft
$C_L$	trim-lift coefficient, $\frac{\text{Lift}}{qS}$
$C_l$	rolling-moment coefficient, $\frac{\text{Rolling moment}}{qSb}$

$C_n$	yawing-moment coefficient, $\frac{\text{Yawing moment}}{qSb}$
$C_Y$	lateral-force coefficient, $\frac{\text{Lateral force}}{qS}$
$C_1$	yaw-damper gain, sec
$G$	transfer function
$I_X$	airplane moment of inertia in rolling, slug-feet <sup>2</sup>
$I_Z$	airplane moment of inertia in yawing, slug-feet <sup>2</sup>
$I_{XZ}$	airplane product of inertia, slug-feet <sup>2</sup>
$\text{Im}$	imaginary part of a complex number
$K$	forward-loop (sensitivity) gain
$K', k'$	roll-rate feedback gain, sec
$K'', k''$	roll-acceleration feedback gain, sec <sup>2</sup>
$K_I$	integrator gain, sec <sup>-1</sup>
$K_X^2 = I_X / mb^2$	
$K_Z^2 = I_Z / mb^2$	
$K_{XZ} = I_{XZ} / mb^2$	
$m$	airplane mass, slugs
$M$	Mach number
$p$	Laplace transform variable
$P$	period of oscillation, sec
$q$	dynamic pressure, slug-feet <sup>-1</sup> -sec <sup>-2</sup>
$\text{Re}$	real part of a complex number
$S$	wing area, ft <sup>2</sup>

$T_{1/2}$	time for an oscillation to damp to half-amplitude, sec
$V$	steady-state velocity of airplane, feet-sec <sup>-1</sup>
$\beta$	airplane sideslip angle
$\gamma$	airplane flight-path angle
$\delta_a$	total aileron deflection, positive in direction to give a positive rolling moment, deg or radians
$\delta_r$	rudder deflection, positive with trailing edge to left, deg or radians
$\epsilon$	error in bank angle ( $\phi_i - \phi$ ), deg or radians
$\lambda_r$	dimensional damping-in-roll root of airplane characteristic equation, sec <sup>-1</sup>
$\mu_b$	airplane lateral relative-density parameter, $\frac{m}{\rho S b}$
$\rho$	air density, slugs-ft <sup>-3</sup>
$\sigma = K_I/K$	sec <sup>-1</sup>
$\tau$	characteristic "time lag" of a first-order lag element in automatic pilot system, sec
$\phi$	airplane bank angle, deg or radians
$\phi_i$	command bank angle, deg or radians
$\psi$	airplane yaw angle, deg or radians
$\omega$	angular frequency, radians-sec <sup>-1</sup>

## Subscripts:

F	filter in autopilot
L	limiting value
p	in stability derivatives represents derivative with respect to $\dot{\phi}_b/2V$
r	in stability derivatives represents derivative with respect to $\dot{\psi}_b/2V$

s	aileron servo
ss	steady state
$\beta$	in stability derivatives represents derivative with respect to $\beta$
$\delta_a$	in stability derivatives represents derivative with respect to $\delta_a$
$\delta_r$	in stability derivatives represents derivative with respect to $\delta_r$

Square brackets around a ratio of two quantities indicate the transfer function relating the quantities.

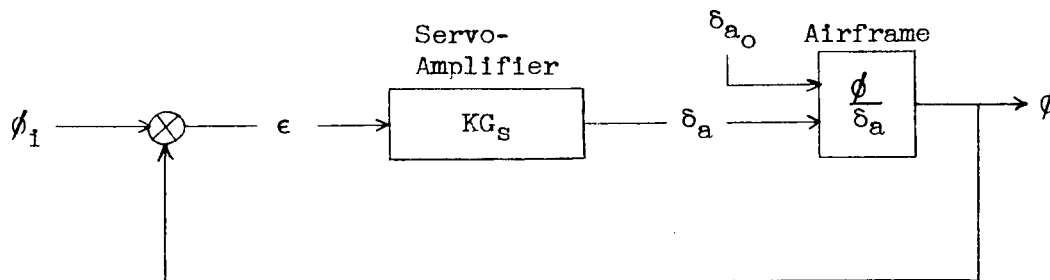
The stability derivatives listed in table I correspond to angular variables in radians.

#### DISCUSSION OF ROLL-CONTROL SYSTEM

In these remarks and in the first part of the analysis, the non-linear effects of limiting the amplitude and rate of aileron motion will be neglected. This assumption should give valid results for small gains in the autopilot system and/or small commands, because the aileron motions may then be assumed to be relatively small so that there would be little or no limiting action. When the linearized equations of lateral motion are used for the airplane, the whole system is linear, and the well-known methods for analyzing and synthesizing linear servo systems may be used. For a discussion of these methods, see reference 1.

#### Basic Roll-Command System

The fundamental roll-command system may be represented by the following block diagram:



The signal  $\phi_i$  is considered to be a command in bank. This command is compared with the actual bank angle, and the difference  $\epsilon$  is amplified and applied to actuate the aileron servomechanism. The transfer function  $KG_s$  represents the amplification of the amplifier and servo and the transfer function of the servo. The amplification  $K$  will be called the forward-loop gain or the sensitivity gain, since it indicates the sensitivity of the control to errors. The resultant aileron deflection should cause the airplane to roll so that the angle of bank  $\phi$  approaches the command in bank  $\phi_i$  as rapidly and as smoothly as possible. It is assumed that the input signal is arbitrary, that is, independent of the aircraft motions. The transient response to a step command input is analyzed to evaluate the desirability of a given control system.

For convenience, the total aileron deflection  $\delta_a$  is defined as positive in the sense that would lead to a positive rolling moment; that is,  $C_{l\delta_a}$  is positive. With this definition, a positive error will give rise to positive rolling of the airplane without requiring the consideration of negative gains in the autopilot. The symbol  $\delta_{a0}$  represents the effective aileron deflection corresponding to an external rolling-moment disturbance, positive in the same sense as  $\delta_a$ .

Command response of the basic system.- If it is assumed that the aileron servo has no lags,

$$G_s = 1$$

and the control equation is

$$\delta_a = K\epsilon = K(\phi_i - \phi) \quad (1)$$

The characteristics of the command response of this simple control system are obtained from the closed-loop transfer function

$$\left[ \frac{\phi}{\phi_i} \right] = \frac{K \left[ \frac{\phi}{\delta_a} \right]}{1 + K \left[ \frac{\phi}{\delta_a} \right]} \quad (2)$$

Here  $\left[ \frac{\phi}{\delta_a} \right]$  is the transfer function giving the roll response of the airplane for an aileron deflection. For simplicity this will hereafter be called the airplane transfer function. It is desired that in the steady state  $\left[ \frac{\phi}{\phi_i} \right]_{ss} = 1$ . For this simple system it can be seen that this can

only occur if  $\left[\frac{\phi}{\delta_a}\right]_{ss}$  is infinite. When  $\left[\frac{\phi}{\delta_a}\right]_{ss}$  is finite, there is a steady-state error in the command response.

The open-loop transfer function for this simple system is

$$\left[\frac{\phi}{\epsilon}\right] = K \left[\frac{\phi}{\delta_a}\right] \quad (3)$$

A convenient method for choosing a desirable gain for the system is to work with the complex plot of  $K \left[\frac{\epsilon}{\phi}\right]$ . The inverse of the open-loop transfer function  $\left[\frac{\epsilon}{\phi}\right]$  is generally a rational function of the Laplace operator  $p$ . The complex plot is obtained by setting  $p = i\omega$  and plotting the real and imaginary parts of  $K \left[\frac{\epsilon}{\phi}\right]$  in the complex plane for positive values of  $\omega$ . In the present case  $K \left[\frac{\epsilon}{\phi}\right] = \left[\frac{\delta_a}{\phi}\right]$  and is simply the inverse of the airplane transfer function. Therefore, it is the rolling characteristics of the airplane itself which will determine whether this simple control system can be satisfactory. The characteristics of several airplanes are compared in the first part of the section entitled "Analysis."

Regulatory response of the basic system.— In addition to the command response of the system, the characteristics of the response to external disturbances are important. External disturbances may be rolling-moment disturbances on the airplane itself or "noise" disturbances on the command signal. Both the noise disturbances and the rolling moments caused by air turbulence are randomly varying functions of time. In order to minimize the effects of such disturbances, it is necessary to know their statistical properties (which are assumed to be invariant with time). It may then be possible to apply the theories of generalized harmonic analysis to design a filter to minimize the random disturbance effects. These statistical problems, however, are outside the scope of this paper and the problems connected with noise filtering are not discussed. There will, however, be some discussion of a method of overcoming the destabilizing effect of a filter the dynamic characteristics of which may be represented by a simple time lag. As mentioned in reference 2, the rather complicated optimum filter which is obtained by application of the theory of generalized harmonic analysis can often be replaced by a very simple filter with little loss of effectiveness. For a simple time-lag filter, the method of stabilization presented should be applicable.

Steady out-of-trim rolling moments may also occur on the airplane. The transfer function for the response to an external rolling moment for the simple system is obtained as follows:

$$\begin{aligned}\phi &= \left[ \frac{\phi}{\delta_a} \right] (\delta_{a0} - KG_s \phi) \\ \left( 1 + KG_s \left[ \frac{\phi}{\delta_a} \right] \right) \phi &= \left[ \frac{\phi}{\delta_a} \right] \delta_{a0} \\ \left[ \frac{\phi}{\delta_{a0}} \right] &= \frac{\left[ \frac{\phi}{\delta_a} \right]}{1 + KG_s \left[ \frac{\phi}{\delta_a} \right]} = \frac{1}{KG_s} \left[ \frac{\phi}{\phi_i} \right]\end{aligned}\quad (4)$$

Equation (4) shows that the steady-state response to an external disturbance is  $\phi_{ss} \approx (\delta_{a0})_{ss}/K$ , since  $\left[ \frac{\phi}{\phi_i} \right]_{ss} \approx 1$ . Therefore, this simple

system has no regulatory stability. That is, as long as external disturbances persist, a steady-state error will exist in the output bank angle of the system. Some modification of the system is needed if it is to be made self-trimming. It should be noted that the magnitude of  $(\delta_{a0})_{ss}$  is likely to be only a few degrees so that the error caused by such steady disturbances would be small, especially for large  $K$ . Nevertheless, a method of obtaining regulatory stability will be discussed.

#### Methods of Improving the Response of the Basic System

Usually, the command response will not be satisfactory for such a simple control system either. However, even when the controlled airplane does have satisfactory rolling-response, the effect of time lags in the servo and/or noise filter will be destabilizing so that some modification of the system will be necessary. For linear systems, the most logical way to approach this problem of modifying the system to obtain desirable dynamic characteristics is to consider the basic system as a network having certain undesirable dynamic characteristics which are revealed in its open-loop response curve or frequency-response curves. A "compensating network" may then be designed which, when inserted into the system, will modify these curves in such a way as to cancel out the undesirable characteristics. When nonlinearities enter into the system, however, it becomes rather difficult to evaluate their effects on the compensating network since the analysis of the nonlinear mechanics of fairly complicated systems presents considerable difficulties.

An alternate approach to the synthesis of a desirable system is the proportional-gain method used in this investigation. In this method the dynamic characteristics of the system are modified by varying the gains on auxiliary inputs to the aileron servo. Although the approach is different, the desired results are the same for this method as for the compensating-network method, namely, to obtain desirable response characteristics for the complete system. This method has the advantage that certain of these gains have a familiar significance to the aeronautical engineer in that they may be interpreted as representing terms in the linearized equations of airplane motion. A more important advantage is that, when nonlinearities enter the system, it is comparatively simple to investigate empirically the effects of varying the gains on the transient response of the nonlinear system by use of an analog computer such as the REAC.

## ANALYSIS

### Linear Roll-Command System

Since the rolling characteristics of the airplane will determine the characteristics of the basic roll-command system, these characteristics are investigated by studying the linearized equations of lateral airplane motion.

Effects of the roll characteristics of the airplane.— The equations of lateral motion of an airplane for small perturbations from equilibrium are

$$2\mu_b K_x^2 \frac{b^2}{V^2} \ddot{\phi} - \frac{1}{2} C_{l_p} \frac{b}{V} \dot{\phi} - 2\mu_b K_{xz} \frac{b^2}{V^2} \ddot{\psi} - \frac{1}{2} C_{l_r} \frac{b}{V} \dot{\psi} - C_{l_\beta} \beta = C_{l_{\delta_a}} \delta_a + C_l \quad (5)$$

$$- 2\mu_b K_{xz} \frac{b^2}{V^2} \ddot{\phi} - \frac{1}{2} C_{n_p} \frac{b}{V} \dot{\phi} + 2\mu_b K_z^2 \frac{b^2}{V^2} \ddot{\psi} - \frac{1}{2} C_{n_r} \frac{b}{V} \dot{\psi} - C_{n_\beta} \beta = C_{n_{\delta_r}} \delta_r + C_n \quad (6)$$

$$-C_L \phi + 2\mu_b \frac{b}{V} \dot{\psi} - \psi C_L \tan \gamma + 2\mu_b \frac{b}{V} \dot{\beta} - C_{Y_\beta} \beta = C_Y \quad (7)$$

The only control effects considered in these equations were the rolling moment caused by the aileron and the yawing moment caused by the rudder. The dot over a symbol represents differentiation with time. The transfer

function  $\left[ \frac{\phi}{\delta_a} \right]$  is obtained by taking the Laplace transform of these equations for zero initial conditions and solving for  $\left[ \frac{\phi(p)}{\delta_a(p)} \right]$  where  $p$  is the Laplace transform variable.

The values of the parameters in these equations for the four cases being compared are given in table I. The three airplanes chosen are considered to be realistic high-speed designs which have certain fundamental differences in their roll properties. The airplane which has very little coupling between its rolling and yaw-sideslip motions will be called case A. The flight condition chosen is that for  $M = 0.9$  at an altitude of 20,000 feet. Cases B and C are for an airplane having a very high  $\left| \frac{\phi}{\beta} \right|$  in its Dutch-roll mode. Case B is for a Mach number of 0.9 and an altitude of 20,000 feet, whereas case C is for a Mach number of 1.6 and an altitude of 50,000 feet. Case C has practically no damping of the Dutch-roll oscillation. Case D is an airplane with a large product of inertia that tends to stabilize the Dutch-roll mode. In this case the Dutch-roll mode has damping comparable with case A and  $\left| \frac{\phi}{\beta} \right|$  roughly half-way between the very low value of case A and the very high values of cases B and C. Figure 1 shows motions of these airplanes in response to a sideslip disturbance of  $2^\circ$  and illustrates the differing characteristics of the three airplanes.

Some general properties of airplane roll-transfer functions.- Application of the Laplace transform to the equations of motion gives the general form of solution

$$\left[ \frac{\phi}{\delta_a} \right] = \frac{a_3 p^3 + a_2 p^2 + a_1 p + a_0}{p(A_4 p^4 + A_3 p^3 + A_2 p^2 + A_1 p + A_0)} \quad (8)$$

The final-value theorem for Laplace transforms, when applied to equation (8), says that the bank angle becomes infinite in the steady-state response to a step aileron deflection. However, for  $\gamma = 0$ , the coefficient  $a_0$  in equation (8) vanishes, and the steady-state value of the bank angle is finite. As mentioned in connection with equation (2), this condition implies that there will be a steady-state error in the command response of the basic roll-control system.

For  $\gamma = 0$ , the theoretical steady value is

$$\left[ \frac{\phi}{\delta_a} \right]_{ss} = \frac{C_{l_{\delta_a}} (l_{\mu_b} C_{n_\beta} + C_{n_r} C_{Y_\beta})}{C_L (C_{n_r} C_{l_\beta} - C_{l_r} C_{n_\beta})} \quad (9)$$

This is usually a very large value since the numerator contains a term with the relatively large factor  $\mu_b$  whereas the denominator is the small factor which is closely connected with the spiral damping of the lateral motion. For zero spiral damping, the steady-state value is the desired infinite value. In general, the spiral mode will have some damping, and a small steady-state error will occur in the command response for  $\gamma = 0$ . The distinction between the cases of infinite or very large steady-state bank angle, however, has little or no physical significance. In the first place, the validity of the linearized equations breaks down for very large motion. Moreover, any practical maneuver is over in a few seconds, whereas the effects of the spiral mode on the motion become important only after a long time. It follows that the true steady state is not as important in the maneuver as the effective steady state which occurs a few seconds after the maneuver is initiated.

This can be seen more clearly if the frequency response obtained from the transfer function  $\left[ \frac{\ddot{\phi}}{\delta_a} \right]$  is considered. If the magnitude of this complex quantity seems to be approaching a finite value as  $\omega$  approaches zero, this value is the effective  $\ddot{\phi}_{ss}$ , and the effective value of  $\phi_{ss}$  is infinite. Figure 2 shows a comparison of the frequency responses  $\left[ \frac{\ddot{\phi}}{\delta_a} \right]$  for the four cases when  $\gamma = 0$ . All four curves show that  $\left| \frac{\ddot{\phi}}{\delta_a} \right|$  does seem to approach a finite value at the low frequencies. The sudden drop to zero at  $\omega = 0$ , which is caused by the spiral damping, occurs only at the extremely low frequencies. This amplitude change is accompanied by a  $90^\circ$  shift in phase. Since the break frequency is around  $\omega = 0.1$ , which corresponds to a period of approximately 60 seconds, it is clear that the spiral mode can have no important effect on maneuvers lasting less than 5 or 10 seconds.

The approximate effective steady-state value of  $\left| \frac{\ddot{\phi}}{\delta_a} \right|$  can be calculated fairly simply. In equation (8), if  $\gamma = 0$ , then  $a_0 = 0$ ; and neglecting the spiral damping gives  $A_0 = 0$ , so that  $\left| \frac{\ddot{\phi}}{\delta_a} \right|_{ss} = \frac{a_1}{A_1}$ . From the equations of motion,

$$\left| \frac{\ddot{\phi}}{\delta_a} \right|_{ss} \approx - \frac{2V}{b} \frac{C_{l\delta_a}}{C_{lp} + 2C_{LKxz} + \frac{C_{l\beta}}{C_{np}} (2C_{LKz}^2 - C_{np})} \quad (10)$$

Equation (10) is obtained by considering only those terms which have  $\mu_b$  as a factor and yields a very good approximation. The effective

steady-state values obtained from equation (10) for cases A, B, C, and D, respectively, are 11.8, 21.2, 42.5, and 27.7 in units of degrees per second per degree. From figure 2, it can be seen that these values are an excellent approximation of the effective steady-state magnitudes at low frequencies. Some unpublished work by Leonard Sternfield of the Langley stability analysis section has shown that this expression also gives excellent agreement when compared with flight records of a number of airplanes in various flight conditions.

The previous discussion has shown that the effects of spiral damping may be ignored in considering the dynamic rolling characteristics of an airplane for maneuvers of reasonably short duration. In fact, in order to obtain realistic results for effective steady-state values, it is necessary to ignore the spiral damping. In order to investigate the effects of flight-path angle,  $\gamma$ , the  $\left[\frac{\ddot{\phi}}{\delta_a}\right]$  response was calculated for case D with  $\gamma = \pm 45^\circ$ . These checked the response for  $\gamma = 0$  almost perfectly for  $\omega > 0.1$ . Thus, the flight-path angle affects only the true steady-state value of  $\left[\frac{\ddot{\phi}}{\delta_a}\right]$  and has practically no effect on the effective steady state nor on the rest of the airplane frequency response except at very low frequencies. Therefore,  $\gamma = 0$  was assumed throughout the investigation for simplicity.

Comparison of several simplified airplane transfer functions.- Since the effects of  $\gamma$  and the spiral mode may be neglected, it is clear that the airplane transfer function  $\left[\frac{\ddot{\phi}}{\delta_a}\right]$  may be written in a simpler form than that given by equation (8). Any further possible simplification would, of course, be desirable, and this problem will now be discussed.

The most obvious simplification would be to assume that the yaw and sideslip motions have very little effect upon the rolling. The roll equation then becomes

$$2\mu_b K_x^2 \frac{b^2}{V^2} \ddot{\phi} - \frac{1}{2} C_{l_p} \frac{b}{V} \dot{\phi} = C_{l_{\delta_a}} \delta_a \quad (11)$$

and

$$\left[\frac{\ddot{\phi}}{\delta_a}\right] = \frac{C_{l_{\delta_a}} \frac{V}{b}}{2\mu_b K_x^2 \frac{b}{V} p - \frac{1}{2} C_{l_p}} \quad (12)$$

Naturally, such an expression is only valid if the effects of the Dutch-roll mode on the rolling response are negligible. Examination of

figure 2 shows that the Dutch-roll oscillation is actually very important in all the cases except case A. It is the Dutch-roll oscillation which causes the marked peak in the other three curves. Therefore, the simplified expression which is given in equation (12) would not be an accurate simulation of the airplane rolling characteristics.

Since the oscillatory properties of the roll-command system are undesirable, it is reasonable to assume that a yaw damper would be used. As a limiting case, suppose there is enough yaw damping and inertia so that the effect of the yawing on the rolling motion can be ignored. Then the airplane transfer function becomes

$$\left[ \frac{\dot{\phi}}{\delta_a} \right] = \frac{C_{l_{\delta_a}} p \left( 2\mu_b \frac{b}{V} p - C_{Y_{\beta}} \right)}{\left( 2\mu_b \frac{b}{V} p - C_{Y_{\beta}} \right) \left( 2\mu_b K_x^2 \frac{b^2}{V^2} p^2 - \frac{1}{2} C_{l_p} \frac{b}{V} p \right) - C_L C_{l_{\beta}}} \quad (13)$$

Equation (13) is the same as equation (12) for those frequencies where the constant term  $C_L C_{l_{\beta}}$  in the denominator may be ignored. This term has an important effect at the low frequencies, however, so that even for infinite yaw damping the approximation given in equation (12) will break down at the low frequencies. It should be noted that increasing the roll damping  $C_{l_p}$  will improve the approximation to lower frequencies.

Equation (13) shows that equation (12) should be a fair approximation to the airplane roll response when a large amount of yaw damping is used, at least for frequencies around  $\omega = 1$  and higher. The damping of the Dutch-roll oscillation, however, is not the only thing which affects the magnitude of the Dutch-roll peak in the  $\left[ \frac{\dot{\phi}}{\delta_a} \right]$  frequency response, as can be seen by comparing the curves for cases A and D in figure 2. These two cases have approximately the same amount of Dutch-roll damping, but the effect of the Dutch-roll mode on the response of case D is much more important. The reason for this effect can be seen by recalling that case A has a very low  $\left| \frac{\phi}{\beta} \right|$  for the Dutch-roll mode. The numerator of the transfer function  $\left[ \frac{\dot{\phi}}{\beta} \right]$  is the same as that in  $\left[ \frac{\dot{\phi}}{\delta_a} \right]$ , and it contains a

quadratic factor in  $p$  which is exactly the Dutch-roll quadratic which would result if only the yaw and sideslip equations were considered. This quadratic gives an excellent approximation to the Dutch-roll mode when such coupling terms as the  $K_{xz}$  term and  $C_{n_p}$  term of the yawing-moment equation are relatively unimportant. Therefore, for airplanes whose rolling motion is little affected by yaw and sideslip motions, the

numerator of the transfer function  $\left[\frac{\phi}{\beta}\right]$  almost vanishes when evaluated for the Dutch-roll characteristic root. Similarly, in obtaining the frequency responses  $\left[\frac{\phi}{\delta_a}\right]$  or  $\left[\frac{\ddot{\phi}}{\delta_a}\right]$ , although the denominator tends to get small at frequencies near the Dutch-roll frequency, the numerator tends to get small at the same time. In fact, very little error results from simply canceling the Dutch-roll quadratic in the denominator with the quadratic in the numerator. Canceling these quadratics and ignoring the spiral mode results in an equivalent airplane transfer function

$$\left[\frac{\ddot{\phi}}{\delta_a}\right] \approx \frac{C_{l\delta_a} \frac{V^2}{b^2}}{2\mu_b (K_x^2 - K_{xz}^2 / K_z^2) (p - \lambda_r)} \quad (14)$$

where  $\lambda_r$  is the dimensional damping-in-roll root. Comparison of equations (12) and (14) shows that they have the same form; that is,

$$\left[\frac{\ddot{\phi}}{\delta_a}\right] = \frac{A}{p - a}. \quad \text{The difference is that the rolling inertia in equation (12)}$$

is replaced by an equivalent rolling inertia in equation (14), and the damping in roll from the rolling equation only is replaced by an equivalent damping in roll, as obtained from all three equations of motion. For this reason, the expression in equation (12) will be called the simplified airplane transfer function and equation (14) will be called the equivalent transfer function.

Figure 3 shows a comparison of the  $\left[\frac{\ddot{\phi}}{\delta_a}\right]$  frequency responses for the complete airplane, the equivalent case, the simplified case, and for the inclusion of an auxiliary yaw-damper of which the equation of motion for the rudder deflection is

$$\delta_r = -C_1 \dot{\psi} \quad (15)$$

Inasmuch as this yaw damper has no lags, the effect of varying the gain  $C_1$  is the same as varying the yaw-damping term in the yawing equation.

Examination of figure 3 shows that the introduction of the yaw damper does tend to remove the Dutch-roll peak and thus yields a less oscillatory rolling response. However, neither the equivalent nor the simplified expression gives a good approximation for cases B, C, or D. On the other hand, either one of these expressions does give a fair approximation to the roll response when a yaw damper is assumed except at the low frequencies. For case A, either method of simplifying the airplane transfer function gives a very good approximation. There is actually no visible difference between the equivalent and simplified curves in this case.

For airplanes like case A, with little coupling between the roll and yaw-sideslip motions, there is very good cancellation of the Dutch-roll effects in the roll transfer function, and this transfer function may be represented by a very simple first-order expression in  $p$ , such as in equations (12) or (14). When the coupling is more important as in cases B, C, and D, the use of a yaw damper will tend to remove the Dutch-roll effects, and the first-order expressions will provide a fair simulation of the airplane response. On the basis of the cases presented here, there seems to be no advantage to using the equivalent approximation instead of the simplified approximation.

It is interesting to note that, although case D has yaw damping as good as case A and less  $\left| \frac{\dot{\phi}}{\beta} \right|$  than cases B or C, it requires considerably more yaw-damper gain to remove the Dutch-roll effects than any of the other cases. This difficulty arises because the large value of product of inertia in case D, which stabilizes the Dutch-roll mode, also changes both the frequency and damping so much that the previously mentioned cancellation of the Dutch-roll mode in  $\left[ \frac{\phi}{\delta a} \right]$  does not occur. Moreover, the use of the yaw damper has little effect on the poor cancellation properties which are caused by the different resonant frequencies in the numerator and denominator of  $\left[ \frac{\phi}{\delta a} \right]$ . Therefore, the use of product of inertia to stabilize the Dutch-roll mode has the disadvantage that it introduces a large component of Dutch-roll oscillation into the rolling motion. For case D, it can be shown that the amount of yaw damping which is required to remove the Dutch-roll oscillation from the rolling motion is actually larger than that required if  $K_{Y\dot{X}}$  had been zero.

The curves of  $\left| \frac{\dot{\phi}}{\delta a} \right|$  no longer seem to approach a constant for low values of  $\omega$  when the yaw damper is introduced, especially for cases B, C, and D. This condition exists because the yaw damper also increases the spiral damping, and the inherent damping in roll for these cases is relatively low. It can be shown that, when the required roll damping is added in cases B, C, and D, the magnitude of  $\left[ \frac{\dot{\phi}}{\delta a} \right]$  once again seems to approach a constant value at low frequencies.

Application of inverse open-loop analysis to compare the basic-control-system response of the airplanes.- Although the frequency

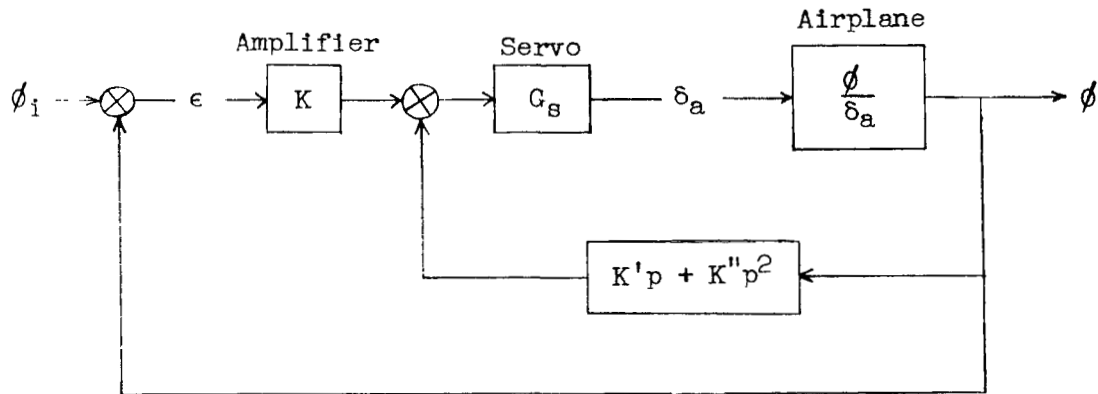
responses  $\left[ \frac{\dot{\phi}}{\delta a} \right]$  give an adequate picture of the dynamic characteristics of the airplane as a rolling system, it was pointed out in the section entitled "Discussion of Roll-Control System" that the complex plot

of  $K \begin{bmatrix} \epsilon \\ \phi \end{bmatrix}$  is more convenient for synthesizing a good roll-control system. Figure 4 shows this plot for the four cases considered. The control system considered is the basic one with  $G_S = 1$  presented previously. Figure 5 shows a comparison for each case of the complex plots of  $K \begin{bmatrix} \epsilon \\ \phi \end{bmatrix}$  for the airplane alone, the equivalent case, and the airplane with yaw damper.

When the standard methods of analyzing these curves (see ref. 1) are applied, it is clear that only case A would yield a satisfactory response when the basic control system discussed previously is used. In particular, the great difference between the effects of the Dutch roll on cases A and D, although both have the same Dutch-roll damping, is evident. The undesirable large loop in the curve for case D is caused by the Dutch-roll mode. The curves of figure 4 indicate that, for case A, with a gain  $K = 0.5$ , the basic system should have a good transient response to a bank command with overshoot somewhere between 1.1 and 1.3 times the command value. For case D, there is no way of choosing a desirable gain, but  $K = 0.5$  seems as good as any. Figure 6 shows a comparison of the transient command responses for these two cases. This comparison clearly shows the superiority of case A when only the basic control system is used. Although this superiority is partly due to the better damping in roll of case A, the product-of-inertia effect is also important. This effect can be seen in figure 7, which shows the effect of the yaw damper when a larger roll damping is assumed in case D. The equivalent approximation is compared with the three-degree-of-freedom representation with and without a yaw damper. The oscillation caused by the Dutch-roll mode is considerable. If there were no product of inertia, the use of the yaw damper would yield a response similar to the equivalent approximation, but, with the product of inertia, the yaw damper has much less effect in removing the oscillation.

The airplane represented by case A has excellent characteristics as a component of a roll command system. From the previous discussion, the important properties seem to be high damping in roll, high Dutch-roll damping, and little coupling between the rolling and yaw-sideslip motions. The fact, however, that case A seems to have a very good roll response with only the simplest type of roll-control system should not be taken to mean that such a simple roll system would really be practical. The flight condition for case A is at a much lower altitude than cases C or D, and it is unlikely that an airplane flying at the altitudes common to present-day interceptors could have sufficient damping in roll or Dutch-roll damping. Moreover, the destabilizing lags inherent in the control and guidance systems would probably have to be compensated for by stabilizing devices in the roll-control system. However, it is felt that the general conclusion which may be drawn is that such an airplane would simplify the problems of the control-system designer and possibly decrease the size and complexity of the necessary control equipment.

Effects of roll-rate and roll-acceleration feedbacks on the response of a roll-command system.— The discussion of airplane rolling characteristics has shown that by proper design of an airplane it is possible to minimize the necessity for auxiliary automatic-stabilization in the roll-command system. However, since it is unlikely that the desired stability can be obtained at high speeds and altitudes, the possibility of auxiliary stabilizing feedbacks must be considered. Suppose that roll-rate and roll-acceleration feedbacks are added to the basic system, as in the following block diagram.



A qualitative picture of the physical effects of the various gains in this autopilot may be obtained by neglecting the servo lag and considering the airplane transfer function to be given by an approximate second-order expression, as in equations (12) and (14). If

$\left[ \frac{\phi}{\delta_a} \right] = \frac{A}{p(p + a)}$ , the open-loop response is

$$\left[ \frac{\phi}{\epsilon} \right] = \frac{AK}{(1 + AK'')p^2 + (a + AK')p} \quad (16)$$

The characteristic equation of this system is

$$(1 + AK'')p^2 + (a + AK')p + AK = 0 \quad (17)$$

Equation (17) shows that the rolling characteristics of the system are those of a simple damped oscillator. The effect of acceleration feedback  $K''$  is to introduce an increment in roll inertia; the effect of rate feedback  $K'$  is to introduce an increment in roll damping; and the sensitivity gain  $K$  introduces a spring constant in roll which does not exist in the airplane alone. The effects of varying these

three gains on the stability of the roll-command system may therefore be approximated by the well-known effects of varying the inertia, damping, and spring constant of an oscillator.

Equation (17) represents the dynamics of what might be called the roll-command mode. Actually, the airplane characteristic modes, of which the Dutch roll is the most significant, are also present. The effects of the Dutch roll may be minimized by adding yaw damping and by increasing the gains in the roll-command system. For example, figure 8 shows the command responses for case D with  $K = 0.5, 2.0$  and  $10.0$ . The results were obtained with a Reeves Electronic Analog Computer (REAC), and both  $\frac{\phi}{\phi_i}$  and  $\frac{\delta_a}{\phi_i}$  are shown as functions of time. As  $K$  increases, the spring constant of the rolling mode increases and the relative effect of the Dutch-roll mode decreases.

The reason that the Dutch roll has less effect at high gains can be seen if the Dutch roll is considered as providing disturbing rolling moments on the basic roll-command system whose characteristics are given by equation (17). As the spring is tightened by increasing the sensitivity gain, the motions caused by the disturbance decrease.

The significant effects of increasing the sensitivity gain on the command response are that the speed of initial response is increased (that is, the rise time is decreased), the initial overshoot increases, and the frequency and number of cycles to damp to half-amplitude of the roll oscillation increase. The motions shown for the gains  $K = 2.0$  and  $K = 10.0$  in figure 8 are impractical, however, since they call for excessively large aileron deflections and velocities. For example, if the command input were a  $60^\circ$  bank, even  $K = 2$  would call for several hundred degrees per second of aileron motion. This motion is far beyond the capabilities of present servos and indicates the importance of a nonlinear analysis which includes the effects of limiting the amplitude and rate of aileron motion. The linear analysis is valuable chiefly for establishing the general trend of the effects of varying the gains but gives reliable results only for low gains and/or small disturbances.

The effect of rate feedback is to improve the damping of the roll-command mode, and the value of  $K'$  really determines the magnitude of  $K$  which can be used. From equation (17) it can be seen that, since the natural damping of the airplane is generally very small for the purposes of automatic control, the ratio  $K'/K$  determines the damping ratio of the roll-command mode. The simple result is that increasing the roll-rate feedback allows the use of a greater sensitivity gain. Figure 9 shows the transient response for  $K = 10$  and  $K' = 0.5$  and may be compared with figure 8(c) to show how the increased damping can enable the use of increased sensitivity. Although it is entirely

unrealistic to assume that the aileron motion remains linear at this high value of sensitivity gain, it is interesting to note the relatively low value of rate feedback which is needed to stabilize the high-gain system according to the linear analysis. In the motions which will be presented later with the rate limiting included, it will be shown that higher rate feedbacks are needed to stabilize lower gain systems. Additional effects of rate feedback in connection with the effects of servo time lag will also be discussed later.

At first sight, it would seem advisable to use the acceleration feedback to decrease the inertia of the rolling airplane, since it would seem that a decrease in the effective inertia would give more rapid response with less overshoot. In figure 10 the  $\frac{\phi}{\phi_1}$  and  $\frac{\delta_a}{\phi_1}$  transients are shown for case D with  $K = 5$ ,  $K' = 0.26$ , and varying  $K''$ . The motions are shown for  $K'' = 0$  and for  $K'' = \pm 0.035$ . In order to appreciate the physical importance of this value, comparison with the value which represents the inertia of the airplane alone is made. From equation (17), this value of  $K''$  is  $0.049 \text{ second}^{-2}$ . A value of  $K''$  of  $0.035$  therefore represents an increment of more than two-thirds the natural inertia of the airplane. Comparison of the three motions shows that for the linear system the use of negative  $K''$  does indeed improve the response by decreasing the effective inertia, whereas increasing the effective inertia causes a slight slowing up of the response and a slightly increased overshoot. However, it should be noted that the use of negative  $K''$  calls for larger and much more rapid aileron motions and indicates that any difficulties which might arise when the rate of aileron motion is limited would be exaggerated by the use of negative  $K''$ . On the other hand, the use of positive  $K''$  would tend to alleviate these difficulties, with little adverse effect on the response.

Effects of first-order time lag.— In all the previous discussions, the effects of lags in the servo-control system have been ignored. The effects of a so-called "simple time lag" in the aileron servo are obtained by considering for the servo transfer function

$$G_s(p) = \frac{1}{1 + \tau_s p} \quad (18)$$

The inverse open-loop response then becomes

$$\begin{aligned} \left[ \frac{\epsilon}{\phi} \right] &= \frac{1 + G_s(K'p + K''p^2) \left[ \frac{\phi}{\delta_a} \right]}{KG_s \left[ \frac{\phi}{\delta_a} \right]} \\ &= \frac{1}{K} \left\{ (1 + \tau_s p) \left[ \frac{\delta_a}{\phi} \right] + K'p + K''p^2 \right\} \end{aligned} \quad (19)$$

The complete transfer function for  $K \begin{bmatrix} \epsilon \\ \phi \end{bmatrix}$  can be easily obtained by multiplying the inverse airplane-alone transfer functions shown in figures 4 and 5 by the factor  $1 + \tau_s p$  to obtain the effects of the servo-lag and adding the terms  $K'p$  and  $K''p^2$ , which affect the imaginary and real parts, respectively. Figure 11 shows the effects of  $\tau_s$  on the airplane-alone complex plots for case A, which has enough inherent damping to give a satisfactory response when there are no lags, and for case C, in which the inherent damping is insufficient. For case C, a yaw damper with gain  $C_1 = 0.6$  has been assumed in order to eliminate the undesirable Dutch-roll effects.

The effect of the servo time lag is destabilizing. For  $\tau_s = 0$ , both cases are stable for any positive value of sensitivity gain. However, the inclusion of the time lag makes the complex plot approach  $270^\circ$  instead of  $180^\circ$  as  $\omega$  becomes infinite, and the roll-command mode becomes unstable for any value of  $K$  higher than the magnitude of the abscissa at which the curve crosses the real axis in figure 11. As the time lag increases, the maximum stable gain decreases. Figure 11(a) shows that small time lags have little effect on a basically well-damped system in the important frequency range, but larger lags are destabilizing.

In order to compensate for the destabilizing effect of the time lag, it is reasonable to try to increase the rate feedback. Primarily, the destabilizing effect of  $\tau_s$  appears in figure 11 as a lowering of the ordinate at each frequency. From equation (19) it can be seen that increasing  $K'$  will raise the ordinate at each frequency by the amount  $K'\omega$  when the substitution  $p = i\omega$  is made.

Figure 12 shows the effect of varying the rate feedback for two values of time lag. It might be noted, parenthetically, that the curve for  $\tau_s = 0.03$ ,  $K' = 0.1$  is very similar to the curve for  $\tau_s = 0.03$  for case A in figure 11(a). The addition of a yaw damper and some roll-rate feedback has therefore made the response of case C very similar to the response of case A for the airplane alone. This type of result has led some automatic-control enthusiasts to believe that the aerodynamic stability characteristics of an automatically controlled airplane are unimportant, since good stability characteristics can be obtained by use of additional automatic equipment. The trouble with this approach is that it can cause the amount of gadgetry to snowball and an attendant increase in unproductive weight and decrease in reliability. However, in the present investigation the engineering difficulties which might be involved in installing various types of feedbacks and auxiliary inputs will be ignored. The primary emphasis will be to point out what advantages various types of gadgetry may provide.

The results presented in figure 12 show that a system which has been destabilized by a large time lag in the servo can be stabilized by using roll-rate feedback alone. However, the type of response with the combination of high lag and rate feedback is somewhat different from the low-lag case. In the complex plots the chief differences are the high peak which appears in the high-lag case and the fact that the curve crosses the real axis at a smaller magnitude of  $\text{Re} \left[ \frac{Kc}{\phi} \right]$  than for

low time lag. Thus, the permissible sensitivity gains are kept down, and the closed-loop frequency response for a desirable sensitivity gain setting would exhibit a pronounced dip at frequencies somewhat below the peak frequency and a sharper peak; thus, there is an increased rise time and a tendency to high-frequency oscillation. From equation (19) it can be seen that it might be desirable to include acceleration feedback  $K''$  when large time lags exist. The contribution of the acceleration feedback  $-K\omega^2$  would tend to increase the magnitude of the real components of the complex plot. The effect would be to smooth out the peak due to  $K'$  and also move the crossing point further out on the real axis, so that higher gains may be used. For example, figure 13 shows the effect of acceleration feedback corresponding to an increase of effective inertia on the curve with the highest peak in figure 12. Comparison of figures 12 and 13 indicates that the combination of roll-rate and acceleration feedbacks does a better job of canceling the effects of high time lag and providing the same type of complex plot as was obtained for the low-time-lag cases.

Figure 14 shows a comparison of calculated time histories of the command response  $\frac{\phi}{\phi_1}$  for the cases of no acceleration feedback and

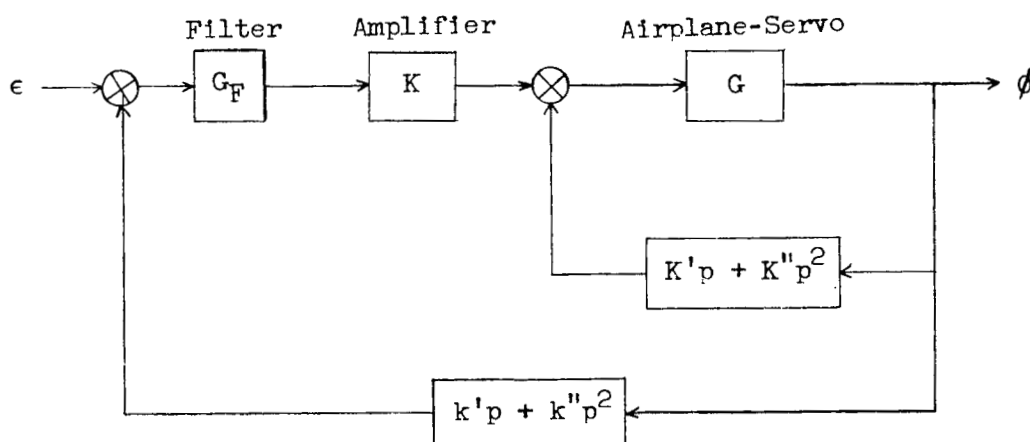
$K'' = 0.05$ , the complex plots of which are shown in figure 12. Sensitivity gains were chosen which would give the same peak amplitude in both frequency responses. Figure 14 shows the possible advantage of using acceleration feedback along with the rate feedback to compensate for the time lag. The effects of the dip and peak which occur in the frequency response when only rate feedback is used can be seen in the transient response as a delay in the initial rise and a high frequency oscillation. The fact that acceleration feedback has a beneficial effect on the response of the linear system with time lag is particularly interesting because it will be shown later that this type of feedback is very important when control-rate limiting exists.

In practice, modern high-performance servos have low time lags. The value of  $\tau_s = 0.03$  second was assumed for the investigation of the effects of aileron deflection and velocity limiting which was carried out on the REAC. The previous discussion has shown that this small time lag has no important effect on the response characteristics when the basic system has satisfactory damping. It would therefore seem unnecessary

to consider the use of rate or acceleration feedbacks to counteract the time-lag destabilization. However, other parts of the guidance system, such as the radar, computer, or noise filter, might easily have time lags higher than 0.3 second. Such time lags have been shown to have a very strong destabilizing effect on the system, and in this case stabilizing feedbacks would be necessary. It should be noted, however, that, in order to get the results shown in the previous figures, the feedback must be applied at a point before the part of the system

which has the time lag. For example, let  $G(p) = \frac{[\phi/\delta a]}{1 + \tau_s p}$  represent

the airplane transfer function with servo lag included. Consider a noise filter placed as in the following block diagram, with extra stabilizing feedbacks fed in before the filter.



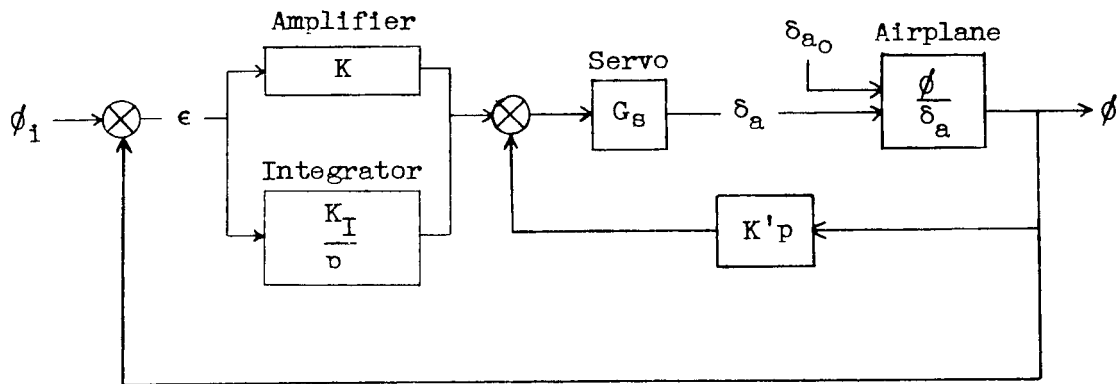
If the filter may be represented by a simple-time-lag transfer function of the form  $G_F = \frac{1}{1 + \tau_F p}$ , the inverse open-loop transfer function becomes

$$\left[ \frac{\epsilon}{\phi} \right] = \frac{1}{K} \left\{ (1 + \tau_F p) [G^{-1}(p) + K'p + K''p^2] + K(k'p + k''p^2) \right\} \quad (20)$$

It has been shown that the servo time lag in  $G(p)$  can be compensated for by use of  $K'$  and  $K''$ , especially since the servo time lag is small. Then the inverse transfer function of the inner loop  $[G^{-1}(p) + K'p + K''p^2]$  has a complex plot very like that of the no-lag system. From a comparison of equations (19) and (20), it can then be seen that  $k'$  and  $k''$  will have the same effect in eliminating the destabilization caused by the time lag  $\tau_F$  as  $K'$  and  $K''$  had on the destabilizing effect of  $\tau_s$  in the simpler system. Therefore, the rate and

acceleration feedback gains  $k'$  and  $k''$ , which control the stabilizing feedback which comes in before the filter, can be used to compensate the filter-time-lag effect in exactly the same manner as  $K'$  and  $K''$  were shown to compensate the servo time-lag effect.

Effect of error integration.— None of the systems previously discussed have an integrator in the forward loop, and, therefore, they all have a small steady-state error in the command and regulatory responses. If an integrator were placed in series with the amplifier, it would introduce a destabilizing phase shift very similar to that which occurs for the filter which has just been discussed, when the time constant of the filter is very large. It is possible to avoid this extreme destabilizing effect and still retain the steady-state effects of the integrator by placing it in parallel with the amplifier, as in the following diagram.



Here  $K_I$  is the integrator gain.

If we define  $\sigma$  as the ratio of the integrator gain to the sensitivity gain  $K_I/K$  the inverse open-loop transfer function of this system is

$$\left[ \frac{\epsilon}{\phi} \right] = \frac{1}{K} \frac{p}{p + \sigma} \left\{ G_S^{-1}(p) [\delta_a / \phi] + K'p \right\} \quad (21)$$

The effect of introducing the integrator is to multiply the inverse open-loop transfer function by the factor  $\frac{p}{p + \sigma}$ . At high frequencies this factor approaches unity, and the integrator has little effect. At low frequencies the combination of the amplifier and integrator acts like a pure integrator so that there is no steady-state error. There is no steady-state angle of bank in response to a constant external rolling moment either, as can be seen from the regulatory transfer function

$$\left[ \frac{\phi}{\delta_{a_0}} \right] = \frac{p [\phi / \delta_a]}{p + (K'p^2 + Kp + K_I)G_S(p) [\phi / \delta_a]} \quad (22)$$

Therefore, the system with the integrator has regulatory stability and zero steady-state error in command response.

However, the integrator also has some undesirable effects on the command-response characteristics. Figure 15 shows the inverse open-loop responses for case C with  $C_1 = 0.6$ ,  $\tau_s = 0.03$ , and  $K' = 0, 0.1$ , and  $0.3$  and also shows the effect of increasing  $\sigma$  on the two cases with roll-rate feedback. It can be seen that increasing  $\sigma$  is destabilizing inasmuch as increasing  $\sigma$  tends to make the curves approach the curve for no rate feedback. Also, the presence of the integrator causes a  $90^\circ$  phase shift of the curves at frequencies near zero. This change in phase causes the reversed curvature at low frequencies, which causes the magnitude of the frequency response of the closed-loop transfer function to increase rapidly from unity at very low frequencies.

The fact that the magnitude of  $\left[ \frac{\phi}{\phi_i} \right]$  remains considerably greater than unity to very low frequencies indicates that in the transient response  $\phi$  will remain greater than  $\phi_i$  for a relatively long time. That is, the command response will tend to overshoot and approach  $\phi_i$  rather slowly.

It would seem that the relative importance of the effects of the integrator at low frequencies can be decreased by using a higher combination of  $K$  and  $K'$ . Figure 16 shows the effects of  $\sigma$  on calculated transients for different combinations of  $K$  and  $K'$ . The value of  $K = 0.5$  was chosen for  $K' = 0.1$  in order to give a moderate overshoot response when  $\sigma = 0$ . Because of the low gain and high yaw damping, the steady-state error is somewhat over 1 percent. Inserting the integrator, with values  $\sigma = 0.5$  and  $\sigma = 1.0$ , the results predicted from figure 15 may be observed: that is, the overshoot increases, the response is slightly more oscillatory, and the response-time is increased. For the higher value of damping feedback  $K' = 0.3$ , the value  $K = 2.8$  gives approximately the same overshoot as is obtained with the lower values of  $K$  and  $K'$  when  $\sigma = 0$ . When  $\sigma = 0.5$  is introduced, the overshoot is less than that in the low-gain case and the return is considerably more rapid. Thus, the adverse low-frequency effects of the integrator do seem less troublesome when higher sensitivity gain is used.

For the purpose of improving the command response, it is clear that the integrator has a harmful effect, since it introduces an overshoot. The integral is basically useful to eliminate bias errors, such as might

arise from a steady disturbing rolling moment. The steady-state command error may also be interpreted as a bias error. Since these bias errors may theoretically be made negligible by the use of higher gains, it would seem that the use of an integrator introduces unnecessary difficulties. However, in the presence of noise the use of high gains is known to be undesirable. The integrator, on the other hand, has the desirable property of tending to filter the noise, and the undesirable property of tending to saturate in the presence of certain types of noise. This problem of deciding between the use of an integrator or high gain is a general one which arises in the design of all linear automatic control and guidance systems. Inasmuch as it depends basically on the noise properties of the system, it is outside the scope of this paper. However, the results presented in figure 16 indicate that, when an integrator is used in a roll-control system, it may be necessary to also use somewhat higher gains in order to decrease the overshoot and slow return caused by the integrator. Thus, some of the desirable properties of the integrator with respect to noise effects may be nullified if it is desired to have a rapid response.

#### Analysis of Results, With Particular Reference to Effects of Control Limiting

The equations of motion of the roll-control system were simulated on the REAC by analoging the lateral equations of airplane motion, given in equations (5), (6), and (7), together with the following aileron control equation for the no-limiting condition

$$\tau_s \dot{\delta}_a = -\delta_a + K(\phi_1 - \phi) + K_I \int_0^t (\phi_1 - \phi) dt - K' \dot{\phi} - K'' \ddot{\phi} \quad (23)$$

The voltages corresponding to the rate of aileron motion and the aileron deflection itself could be limited on both the positive and negative sides. The analog of the limiting mechanism corresponded to a servo which did not have a "wind-up" characteristic; that is, aside from the time lag in the servo, it was assumed that the aileron came off the limits immediately when the input voltage to the servo became less than the limiting value.

When limits are applied to the aileron deflection and rate, the linear differential relation given in equation (23) is replaced by a nonlinear relationship. Therefore, the effects of the limits on the dynamic response of the system depend directly on such things as the relation between the magnitude of the input and the magnitudes of the

limits, and on the relation between the magnitudes of the rate and deflection limits. It is clear that for small enough commands the linear response will always be obtained. Moreover, the response for an input  $\phi_1$  with limits  $\delta_{aL}$  and  $\dot{\delta}_{aL}$  will be exactly similar to the response for an input  $k\phi_1$  with limits  $k\delta_{aL}$  and  $k\dot{\delta}_{aL}$  where  $k$  is an arbitrary constant. This can be seen by considering that the analog of the two problems could be made identical by a simple change of scale factor. By this rule, for example, the response to a command  $\phi_1 = 60^\circ$  with  $\delta_{aL} = 20^\circ$ , and  $\dot{\delta}_{aL} = 120^\circ$  per second is exactly similar to the case of  $\phi_1 = 30^\circ$ ,  $\delta_{aL} = 10^\circ$ , and  $\dot{\delta}_{aL} = 60^\circ$  per second. In setting up the problems it was assumed that the command was a  $60^\circ$  bank angle, and the limiting values are related to this specific command. The motions presented for the  $60^\circ$  bank command were considered to be representative of those which would be obtained in response to fairly large bank commands with the given limits.

Figure 17 shows that, when a fairly high forward loop gain is used in an attempt to get rapid response, even relatively high control limits can have a considerable effect on the system response. The airplane simulated is case A. Figure 17(a) shows the practically linear response obtained when the control limits are set very high. The response is rapid and well damped. Figure 17(b) shows the response for limits  $\delta_{aL} = 20^\circ$  and  $\dot{\delta}_{aL} = 120^\circ$  per second. Although this rate limit is considerably higher than the maximum rates available with present servos, it is seen that the limiting causes some oscillation in the response. Since rate feedback is generally considered the basic stabilizing feedback,  $K'$  was increased, and the motion shown in figure 17(c) was obtained. This motion is seen to be considerably more stable and generally satisfactory. However, it should be noted that there still remains some limiting oscillation, even though the rate feedback is now far higher than would be considered necessary from a linear analysis.

The command response in figure 18(a) shows what happens when the same autopilot with the same limits is applied to case C. Since the value of  $\sigma$  is  $1/3$  in this case, and the rate feedback is high, the results presented in figure 16 indicate that a linear analysis would predict a very well damped motion. Because of the limits, a neutrally stable oscillation actually results. The records of  $\delta_a$  and  $\dot{\delta}_a$  show that this oscillation is caused by the limiting of the aileron rate. Although the record of  $\dot{\delta}_a$  shows its limiting value rather than zero when  $\delta_a$  is limiting, the true value was actually used in computing  $\delta_a$ . Physically, it would be expected that limiting the control rate would be destabilizing, since control-rate limiting introduces a lag in the control motion called for by the linear equations. Figures 18(b) and 18(c) show that increasing the rate feedback is not basically the best method

of eliminating the rate-limiting oscillation. Although the oscillation is stabilized by rate feedback, even the use of extremely high rate feedback which slows up the response very much does not succeed in eliminating the rate-limiting oscillation.

Figure 19 shows the results of varying the control limits. In figure 19(a) the command response is shown for the same autopilot that was used in figure 18(b) except that the rate limit is increased from  $120^\circ$  per second to  $180^\circ$  per second. The result is a considerable improvement in the stability of the limiting oscillation because of the decrease in the amount of lag caused by rate limiting. Although the effects of varying the control-rate limit seem to correspond to varying the effective lag in the roll-control system, the variation of the control-deflection limit would seem to correspond to varying the effective forward-loop gain. The response shown in figure 19(b) shows the effect of changing the limits to  $\delta_{a_L} = 10^\circ$  and  $\dot{\delta}_{a_L} = 120^\circ$  per second. The motion is actually less oscillatory than that shown in figure 19(a). Therefore, the undesirable oscillation caused by rate limiting can be decreased simply by decreasing the deflection limit. The worst condition for the stability of the rate-limiting oscillation can be seen to be that which combines low rate limits with high deflection limits. This result is reasonable, since this condition corresponds to the use of a high effective gain with a high effective lag, both of which should be destabilizing. The stabilizing effect of lower deflection limits has previously been shown in reference 3.

Figure 20 shows the results for the same case with a more realistic rate limit  $\dot{\delta}_{a_L} = 40^\circ$  per second. Although the limit  $\delta_{a_L} = 10^\circ$  now gives neutral stability, as shown in figure 20(a), the motion may again be stabilized by decreasing the limit to  $\delta_{a_L} = 5^\circ$ , as shown in figure 20(b). The method of stabilizing the limiting oscillation by lowering the deflection limit is generally unsatisfactory, however, because this essentially decreases the control effectiveness at large errors and slows up the response. Although the slow-up is rather small for the airplane in case C, probably because of the low rolling inertia of this case, it is generally much more pronounced. Figure 21 shows the pronounced slow up for a typical control system with case A, for example, when the stability of the limiting oscillation is improved by decreasing the control-deflection limit. Generally, the method of decreasing the deflection limit to stabilize the limiting oscillation was found to be inefficient, since the loss of control effectiveness caused the type of slow-up response shown in figure 21(b).

The method of stabilizing the limiting oscillation which was found to be extremely effective in all cases was the use of roll-acceleration feedback. Figure 22(a), for example, shows the effect of acceleration

feedback with  $K'' = 0.1$  on the neutrally stable system of figure 18(a). The use of the acceleration feedback in every case resulted in a smooth motion with the limiting oscillation completely suppressed. The complete elimination of the sawtooth aileron oscillation which occurred in figure 18(a) should be noted. It was found that a relatively wide range of acceleration-feedback gain yielded smooth responses without appreciably slowing up the response in cases where  $K'' = 0$  gave a limiting type of oscillation. However, the use of excessive acceleration feedback, because of the very large increase in effective inertia, caused a slower response and a sluggish oscillation. For example, figure 22(b) shows the motion when the acceleration feedback in figure 22(a) is doubled. It can be seen that a slow, large amplitude oscillation is developing.

The main effects of the integral gain described in the linear analysis were basically unchanged when the runs with control limiting were made. As shown in figures 15 and 16, the only effective method of decreasing the overshoot arising from integral gain was found to be the use of higher combinations of  $K$  and  $K'$ . Also, the steady-state command errors without the integral-gain were not found to be significant, especially for high forward-loop gains. The integral gain might be desirable, however, to give the system regulatory stability, that is, a self-trimming property. Figure 23 presents typical regulatory responses, which show that increasing the integral gain from  $K_I = 1$  to  $K_I = 5$  makes the self trimming occur much more rapidly. The motions are in response to a steady  $C_l = 0.01$ , which corresponds to  $\delta_{a_0} = 8^\circ$  for case A. From equation (4), this system (with  $K = 3$ ) would have a steady error  $\phi = 2.5^\circ$ , if no integral gain were used. The motions in figure 23 show that  $K_I = 1$  gives a rather slow correction of this error, whereas  $K_I = 5$  gives a very rapid correction. Excessive integral gain caused an oscillatory response.

Although the presence of the control limits seems to have no critical effect on the regulatory properties of the integral gain, the integral gain can have a very strong destabilizing effect on the limiting oscillations in command responses. This effect of increasing the integral gain is most evident when the limiting oscillation was originally marginally stable. Figure 24(a) shows the command response corresponding to figure 23(a), with  $K_I = 1$ ,  $\delta_{a_L} = 20^\circ$ , and  $\dot{\delta}_{a_L} = 40^\circ$  per second; and this response appears to be stable but very oscillatory. Figure 24(b) shows the violent limiting instability which occurs when the integral gain is increased to  $K_I = 5$ . In order to verify that the instability is not caused by  $K_I$  alone but rather by the effect of  $K_I$  on the limiting oscillation, figure 25(a) shows the response of the same system with high limits. The motion appears to be very stable and satisfactory. On the other hand, figure 25(b) shows the response for  $K_I = 0$  which

resembles closely the response for  $K_I = 1$ . Thus, moderate values of integral gain have little effect on limiting stability whereas large values cause violent instability. It is not likely, of course, that such high integral gains would be necessary since it is probable that the type of regulation for steady out-of-trim moments shown in figure 23(a) would be satisfactory. The motions in figures 24 and 25 show that the attempt to obtain rapid regulation by use of high integral gain would greatly increase the limiting-oscillation difficulty.

The effects of time lag predicted from the linear analysis also were basically unchanged when limiting occurred. For example, figure 26 shows that the use of rate feedback tends to stabilize the oscillation caused by time lag, but that the combination of rate and acceleration feedback gives better results. The motions in figure 26 are for case C and agree with the results shown for the linear case in figures 13 and 14. In general, good results in stabilizing the time-lag effect for cases A and D were obtained with rate feedback alone. The use of acceleration feedback was probably more important in case C because of the low relative roll inertia of this case.

The destabilizing effect of increased time lag was more evident at low gains than at high gains, as shown in figure 27 for case A. This result seems to contradict the effect found in the linear analysis, that high gains tend to cause oscillatory instability in the presence of time lags. However, in figures 27(c) and 27(d) a very high value of rate feedback is used to stabilize the rate-limiting oscillation, and this high rate feedback counteracts the time-lag effect. In fact, when the linear open-loop plots are drawn for the cases in figures 27(c) and 27(d), the effect of the increased time lag is found to be small in the important frequency range because the system is very much overdamped by the large amount of rate feedback. Also, the small high frequency oscillation in figure 27(d) appears to be caused by the lack of acceleration feedback.

These results again illustrate the similarity between aileron-rate limiting and effective time lag. Although the linear analysis showed that the destabilizing effect of time lag is primarily improved by roll-rate feedback and that some acceleration feedback has a favorable effect, the REAC results show that rate-limiting instability is primarily improved by acceleration feedback and that rate feedback can also be helpful. It would seem, therefore, that good results could be obtained for both time-lag and rate-limiting effects with a feedback network consisting of a rate gyro with lead or an angular accelerometer with lag.

The motions in figure 27 also illustrate another interesting result which was evident in all the runs taken on the REAC. It can be seen that the high-sensitivity cases in this figure do not have a faster rise time than the low-sensitivity cases. The reason is obvious when the  $\delta_a$  motion is examined. Even the low-gain case causes the aileron to

go against the stops at its maximum rate so that no more rapid rise time could possibly be obtained with these limits. Therefore, it would seem desirable to use the lowest sensitivity gain (with associated auxiliary gains) that would cause the aileron to move at maximum velocity throughout the activating pulse for large inputs. In this case there would be little tendency to rate-limiting instability, and the required gains would be close to those predicted from a linear analysis. In this almost linear system, the rise and response times would be practically the same for any magnitude of command. Examples of the desirable type of control motion for various limiting combinations are shown in figures 19(b), 21(b), and 26(a). In these cases, a smooth, low-overshoot response is obtained for the large command input.

However, it is obvious that this type of system would not be optimum since it requires just as long to roll through a small angle as through a large one (as do all linear systems). The maximum capabilities of the system are utilized only for large commands. This objection can be partly overcome by using higher gain combinations, which would provide the desired nonlinear control motions for a larger range of commands, and inhibiting the tendency to limiting oscillations by means of acceleration feedback. Practically however, there would be limits to the use of high gains because the use of too high an acceleration feedback eventually causes a slow-up of the response and also because of noise difficulties with high gains.

The above considerations, however, suggest an entirely different approach to the control problem. It may be possible to determine the desired motion by some approach which ignores the use of gains or feedbacks entirely. It seems physically obvious that the control motion needed is an aileron pulse to start the rolling and a reverse pulse to stop the rolling when the proper angle is reached. If it is assumed that the aileron servo is velocity-limited, it seems reasonable that the most rapid response would be obtained if the control were moved at maximum velocity throughout the motion. The desired control motion would then consist of two triangular pulses, very much like that shown in figure 26(a). For some conditions one or both triangular pulses might be truncated, as in figure 19(b). With this type of control motion assumed, it is only necessary to calculate the timing parameters of the aileron pulse as a function of input command magnitude. In an unpublished analysis, this has actually been done by using the simplified roll transfer function. Such a system is completely nonlinear and open-loop, although the loop could be closed after each aileron pulse to sample the error. A more complete discussion would be out of place in the present paper, but this brief description has been presented for two reasons. First, it indicates that it may be possible to use nonlinear systems which take advantage of the rate-limiting property which is so troublesome in linear systems. Secondly, this type of system might be used for large roll commands in conjunction with a

linear system for small commands. By using the linear system for small commands only, it becomes much simpler to design a high-sensitivity, rapid-response system without getting involved in limiting difficulties.

## CONCLUSIONS

The dynamic characteristics of several modern high-speed fighter airplane configurations as automatic roll-controlled systems have been compared. The type of autopilot investigated was a proportional-gain autopilot that controlled the error in bank angle. It was found that there were important differences in the dynamic characteristics of these airplanes as roll-controlled systems. Desirable airplane-stability characteristics were found to be high damping in roll, high Dutch-roll damping, and little coupling between the rolling and yaw-sideslip motions. Inclination of the principal axis to the flight path in order to stabilize the Dutch-roll oscillation has the undesirable property that it introduces a large component of Dutch-roll oscillation into the rolling motion.

The effect of the forward loop (or sensitivity) gain is to introduce a spring-constant type of moment which results in a characteristic oscillation in roll. The roll-rate feedback gain stabilizes this oscillation. Time lags in the control system are destabilizing, but the effect of a simple time lag can be very well compensated for by the use of a combination of rate and acceleration feedbacks.

Unless an integrator is included in the forward loop, there will generally be small steady-state errors in both the command and regulatory responses. The inclusion of an integrator, however, tends to destabilize the rolling oscillation and cause a large initial overshoot. These effects may be decreased by simultaneously increasing the sensitivity and rate-feedback gains, but some overshoot is inevitable with a system including an integrator.

From the comparison between the results obtained on the Reeves Electronic Analog Computer in which the deflection and rate of deflection of the ailerons were both limited and the results of linear analysis, it seems that the deflection limit acts roughly as a limit of the forward-loop gain in a linear system and the rate limit acts roughly as a time lag. The rate limit introduces a tendency to neutrally stable oscillations in the system in which the ailerons perform a sawtooth oscillation at a maximum rate. The use of a small amount of acceleration feedback was found to be very effective in eliminating this oscillation without slowing up the response considerably. The use of rate feedback and the decrease of the deflection limit were also found to be helpful in eliminating rate-limiting oscillation. The introduction of relatively high integral gain, such as would be required to obtain rapid regulatory

response, caused the rate-limiting oscillation to become violently unstable. However, smaller amounts of integral gain had little effect on the limiting oscillation.

With control limiting, the ability to obtain faster response by increasing the sensitivity gain is limited. Moreover, large sensitivity gains increase the tendency to limiting oscillation for large inputs. If too large sensitivity gains are used, it is therefore necessary to use considerably more rate feedback than would be predicted from a linear analysis, in order to stabilize the system for large inputs. The system then tends to be too slow in the linear range with small inputs. The sensitivity gain should therefore not be so large as to require (in the presence of control-rate limiting for large inputs) considerably more rate feedback than is predicted as desirable from a linear analysis.

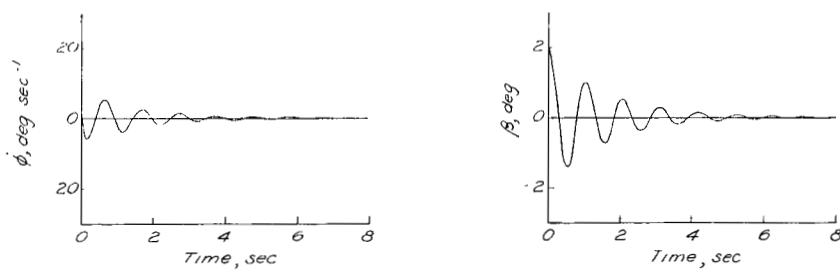
Langley Aeronautical Laboratory,  
National Advisory Committee for Aeronautics,  
Langley Field, Va., May 17, 1955.

## REFERENCES

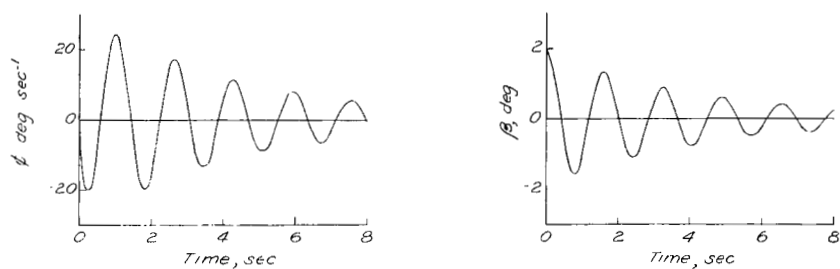
1. Chestnut, Harold, and Mayer, Robert W.: Servomechanisms and Regulating System Design. Vol. I, John Wiley & Sons, Inc., 1951. Ch. 9.
2. Wiener, Norbert: Extrapolation, Interpolation, and Smoothing of Stationary Time Series With Engineering Applications. Appendix B, The Technology Press, M.I.T., and John Wiley & Sons, Inc., 1949.
3. Matthews, Howard F., and Schmidt, Stanley F.: A Theoretical Study of the Effect of Control-Deflection and Control-Rate Limitations on the Normal Acceleration and Roll Response of a Supersonic Interceptor. NACA RM A53B11, 1953.

TABLE I.- MASS AND AERODYNAMIC PARAMETERS FOR  
FLIGHT CONDITIONS CONSIDERED

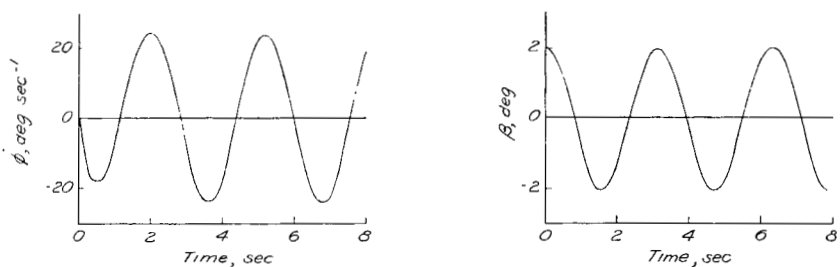
	Case A	Case B	Case C	Case D
Mach Number	0.9	0.9	1.6	1.4
Altitude, ft	20,000	20,000	50,000	60,000
V, ft. sec <sup>-1</sup>	933	933	1,553	1,359
S, ft <sup>2</sup>	288	175	175	401
b, ft	37	25	25	35.8
V/b sec <sup>-1</sup>	25.2	37.3	62.1	38.0
C <sub>L</sub>	0.084	0.138	0.184	0.32
$\mu_b$	30.8	74.5	275	256
I <sub>X</sub> , slug-ft <sup>2</sup>	7,160	3,230	4,240	17,620
I <sub>Z</sub> , slug-ft <sup>2</sup>	22,900	33,900	37,500	122,500
I <sub>XZ</sub> , slug-ft <sup>2</sup>	414	804	1,090	-23,300
C <sub>n<sub>r</sub></sub>	-0.19	-0.65	-0.51	-0.69
C <sub>l<sub>r</sub></sub>	-0.024	-0.17	0.122	0.189
C <sub>n<sub>p</sub></sub>	0.012	0.002	-0.017	-0.014
C <sub>l<sub>p</sub></sub>	-0.37	-0.335	-0.25	-0.275
C <sub>n<sub><math>\beta</math></sub></sub>	0.15	0.218	0.087	0.345
C <sub>l<sub><math>\beta</math></sub></sub>	-0.04	-0.11	-0.057	-0.128
C <sub>Y<sub><math>\beta</math></sub></sub>	-0.77	-0.87	-0.726	-0.785
C <sub>l<sub><math>\delta_a</math></sub></sub>	0.086	0.10	0.10	0.117
C <sub>n<sub><math>\delta_r</math></sub></sub>	-0.10	-0.10	-0.10	-0.10
T <sub>1/2</sub> , sec; spiral mode	100	45	46	131
T <sub>1/2</sub> , sec; damping-in-roll	0.115	.19	0.59	1.40
T <sub>1/2</sub> , sec; Dutch-roll	1.12	3.07	630	1.71
P, sec; Dutch-roll	1.02	1.63	3.14	1.53
$ \phi/\beta $	0.64	6.09	5.77	3.55
Argument $[\phi/\beta]$ , deg	29.4	18.6	24.9	2.1



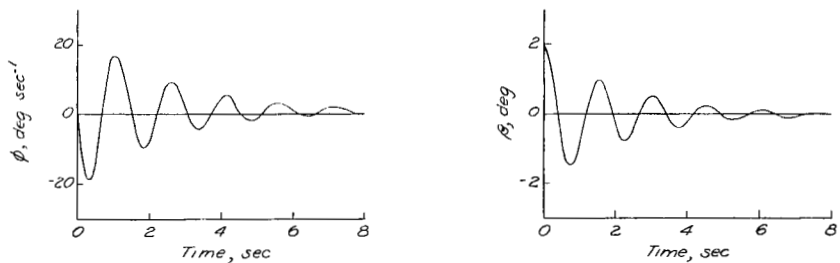
(a) Case A.



(b) Case B.



(c) Case C.



(d) Case D.

Figure 1.- Rolling and sideslip motions of cases A, B, C, and D in response to an initial sideslip disturbance.

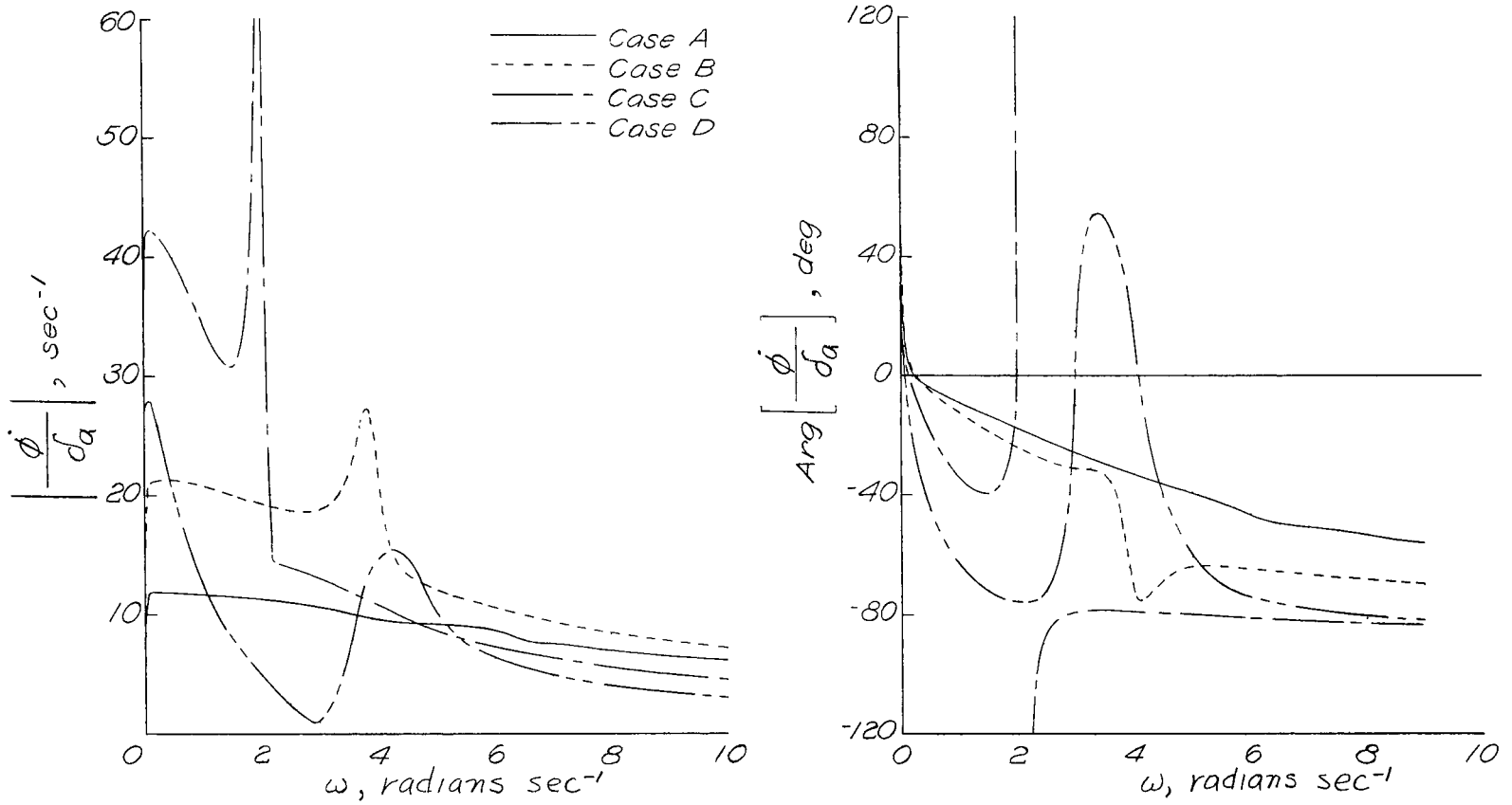
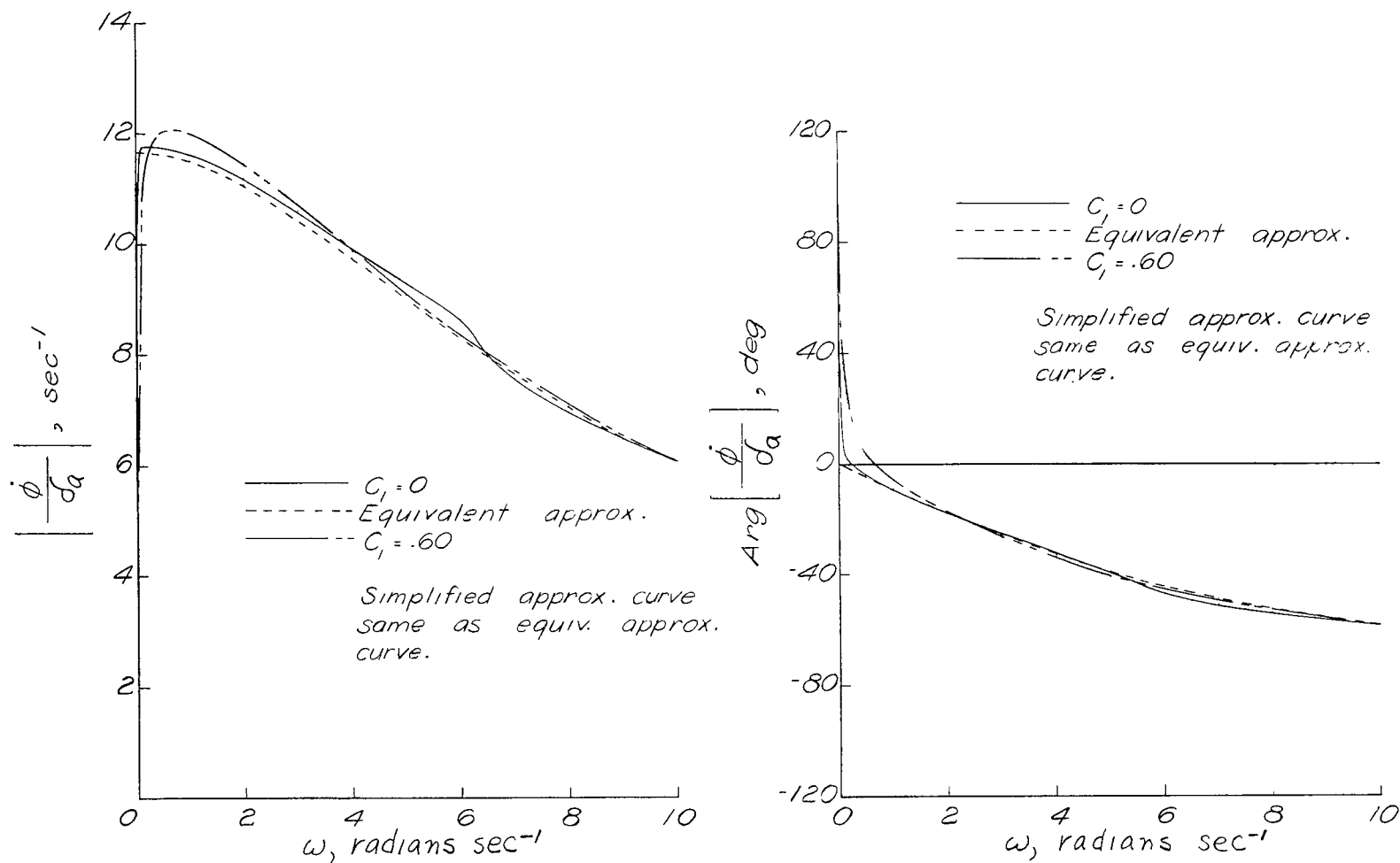
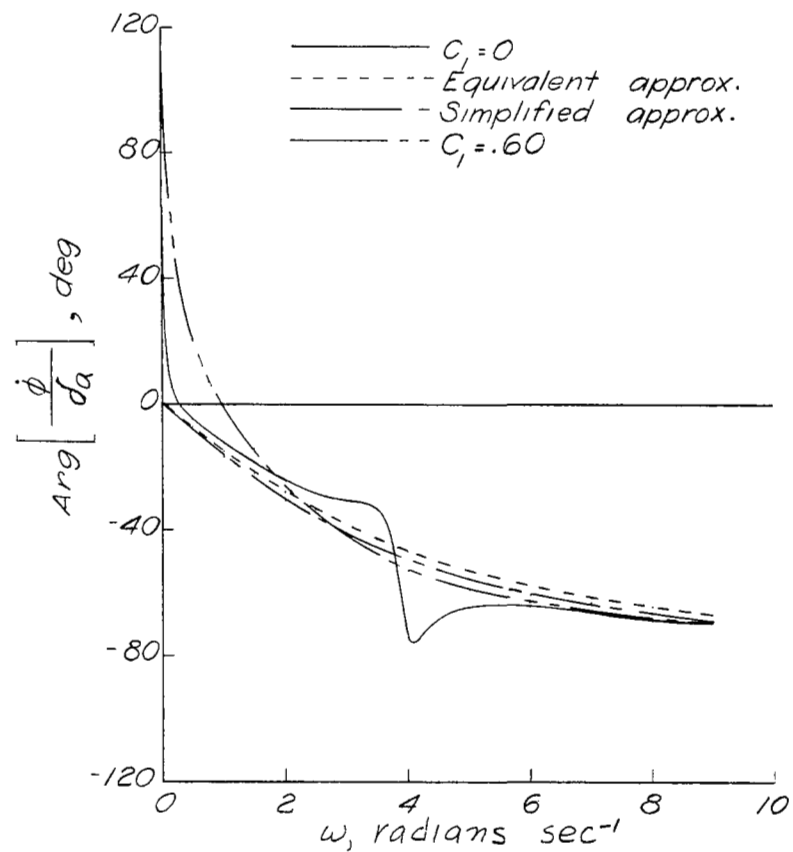
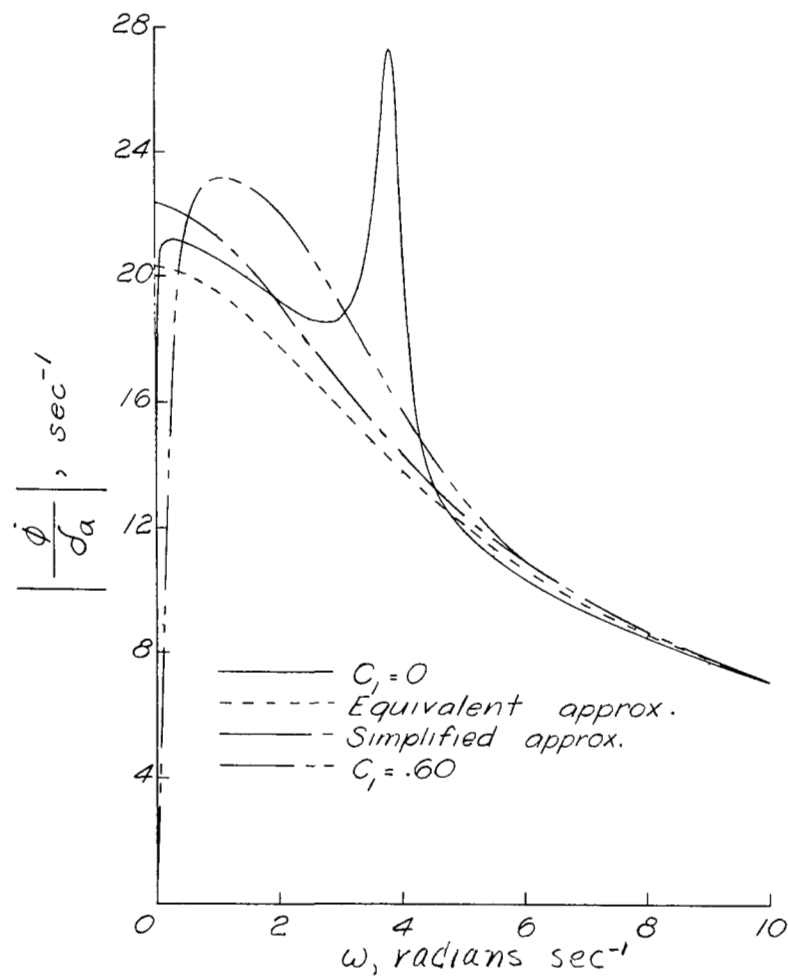


Figure 2.- Frequency responses  $\left[ \frac{d\phi}{d\alpha} \right]$  for the four airplane configurations.  
 $\gamma = 0$ .



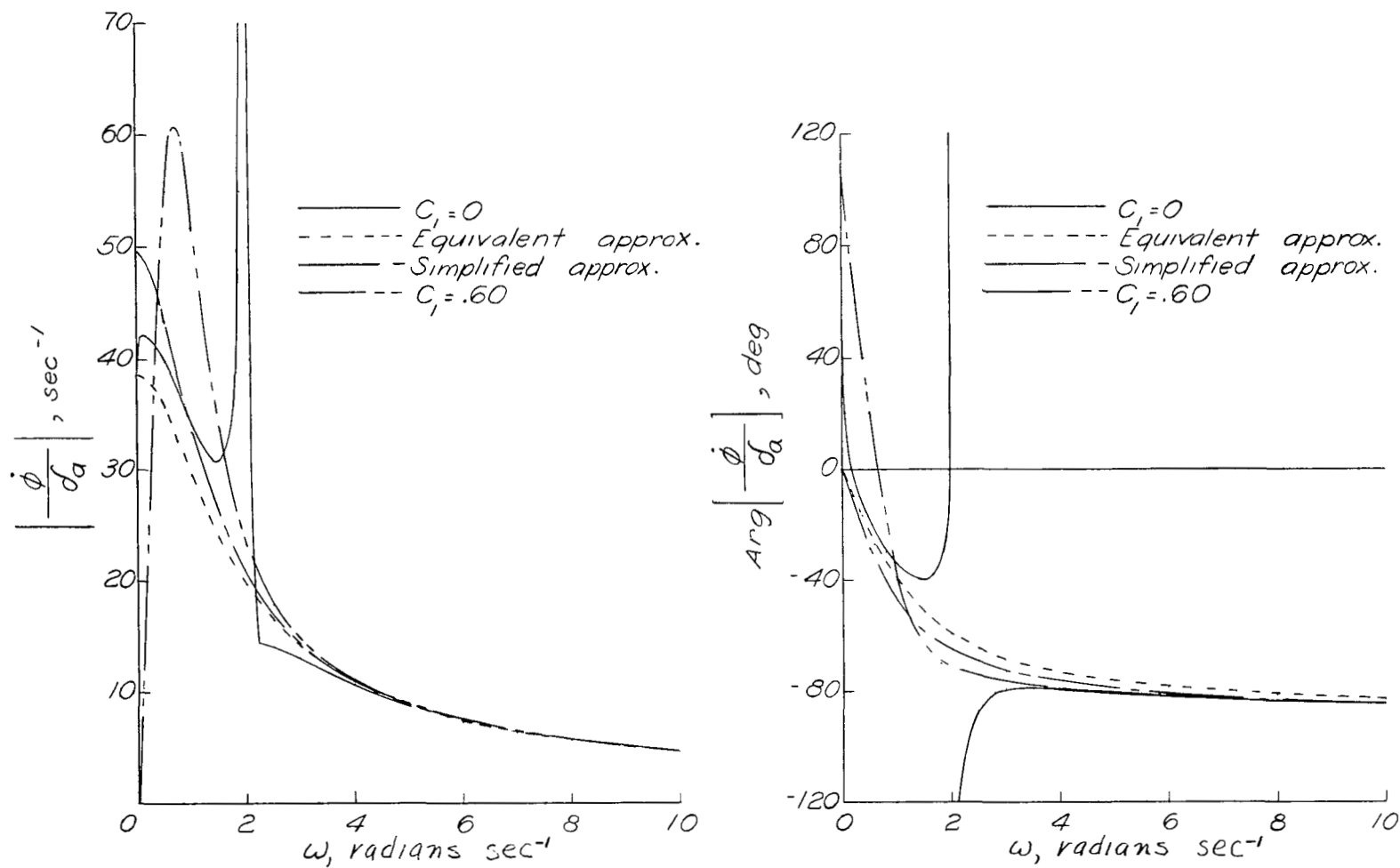
(a) Case A.

Figure 3.- Effect of yaw damper on frequency response in roll and comparison with one-degree-of-freedom approximations.



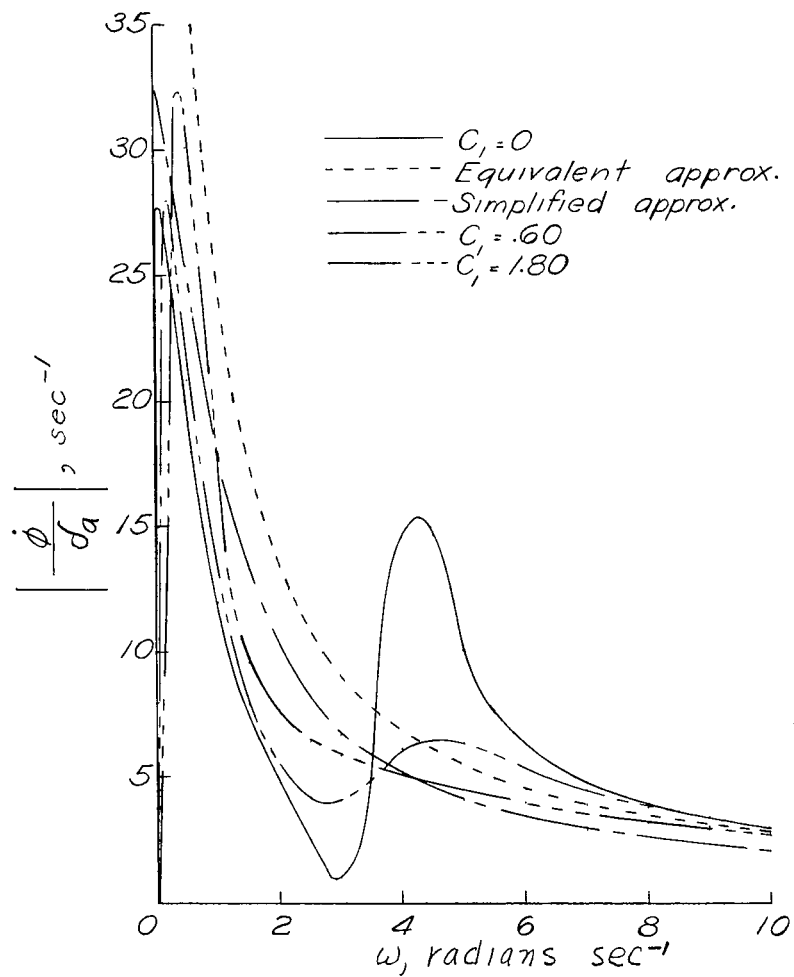
(b) Case B.

Figure 3.- Continued.



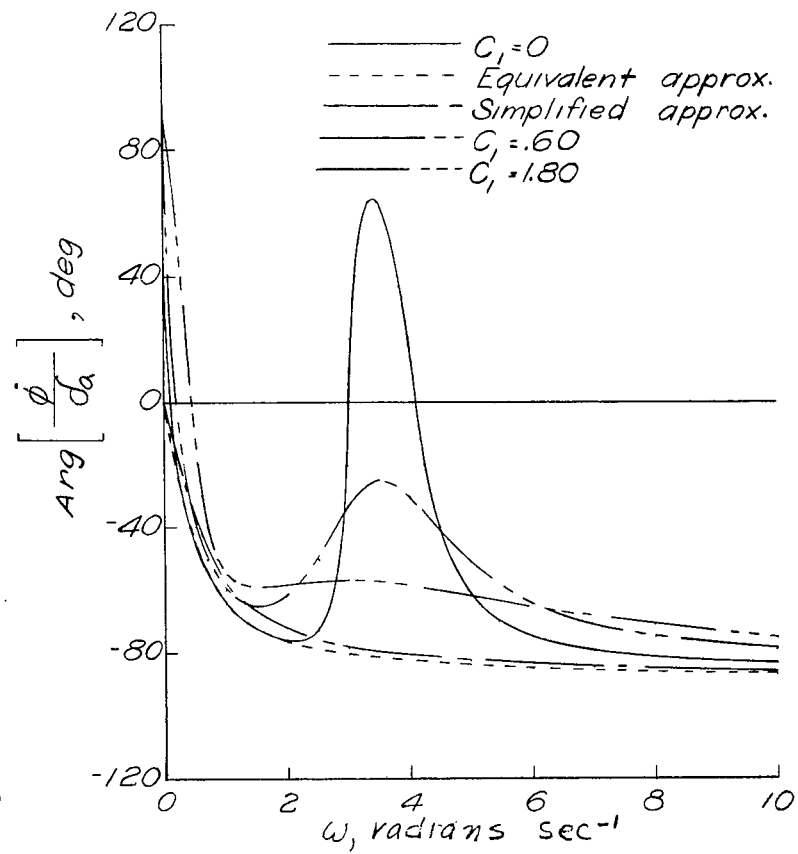
(c) Case C.

Figure 3.- Continued.



(d) Case D.

Figure 3.- Concluded.



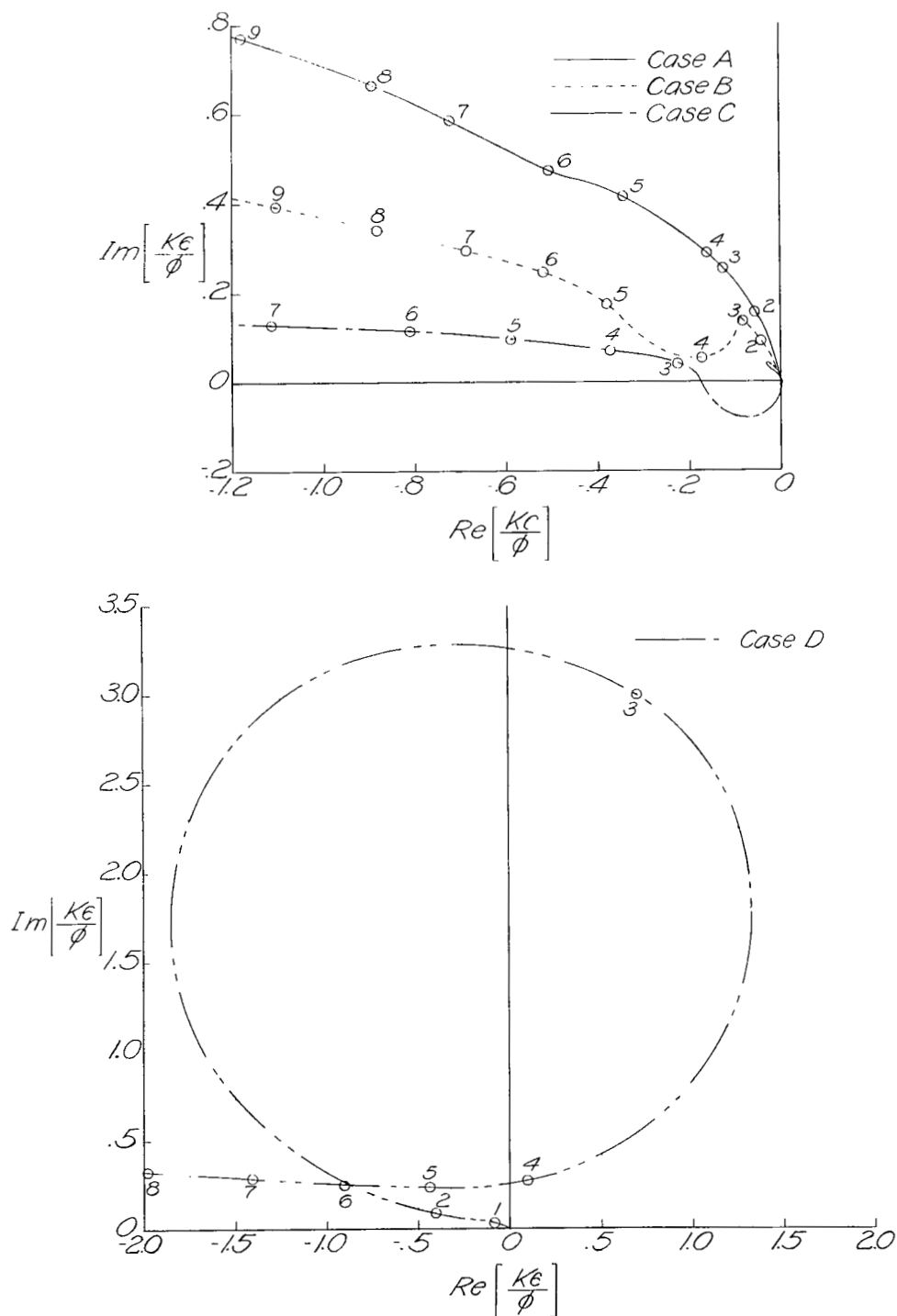
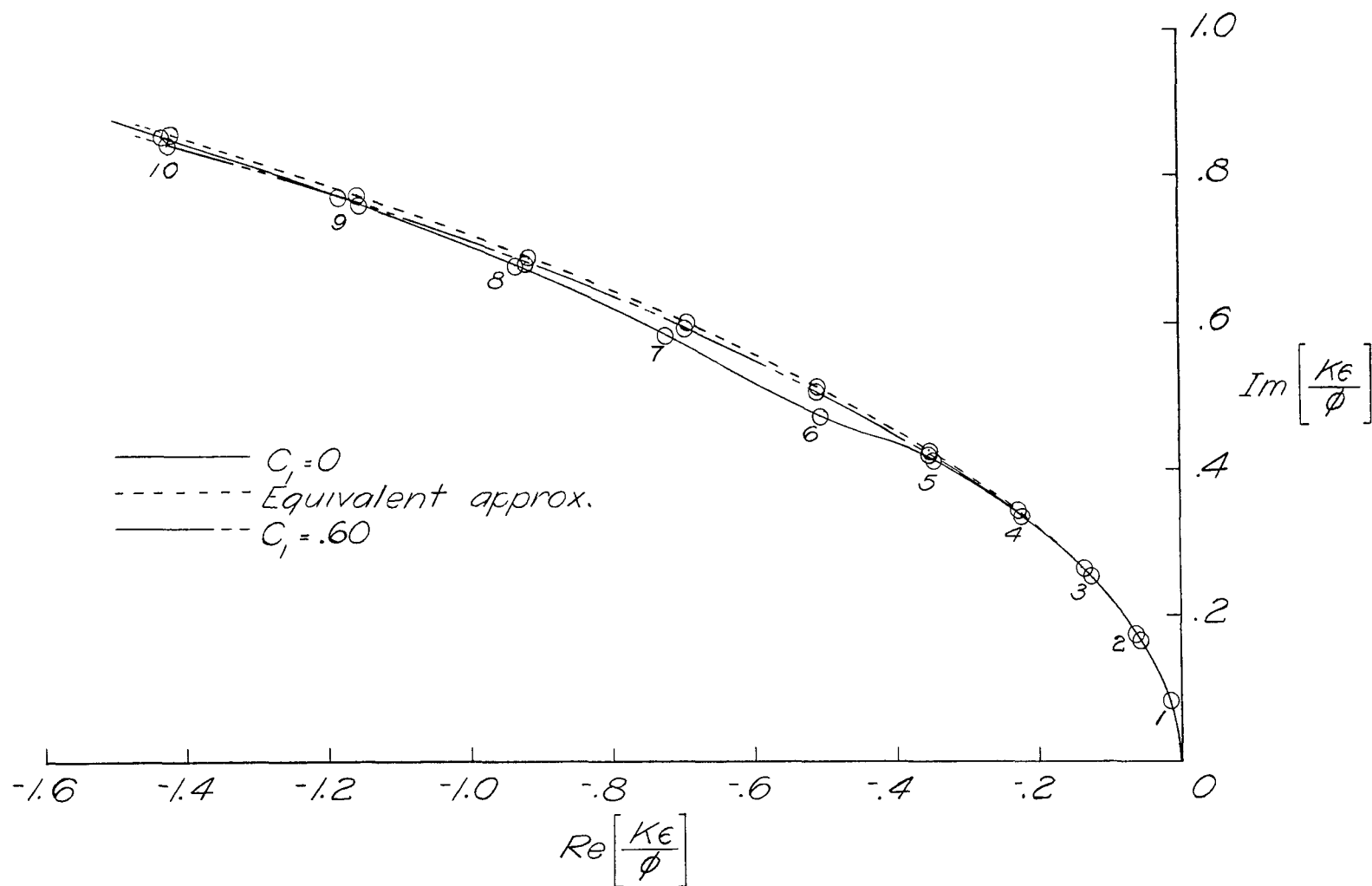
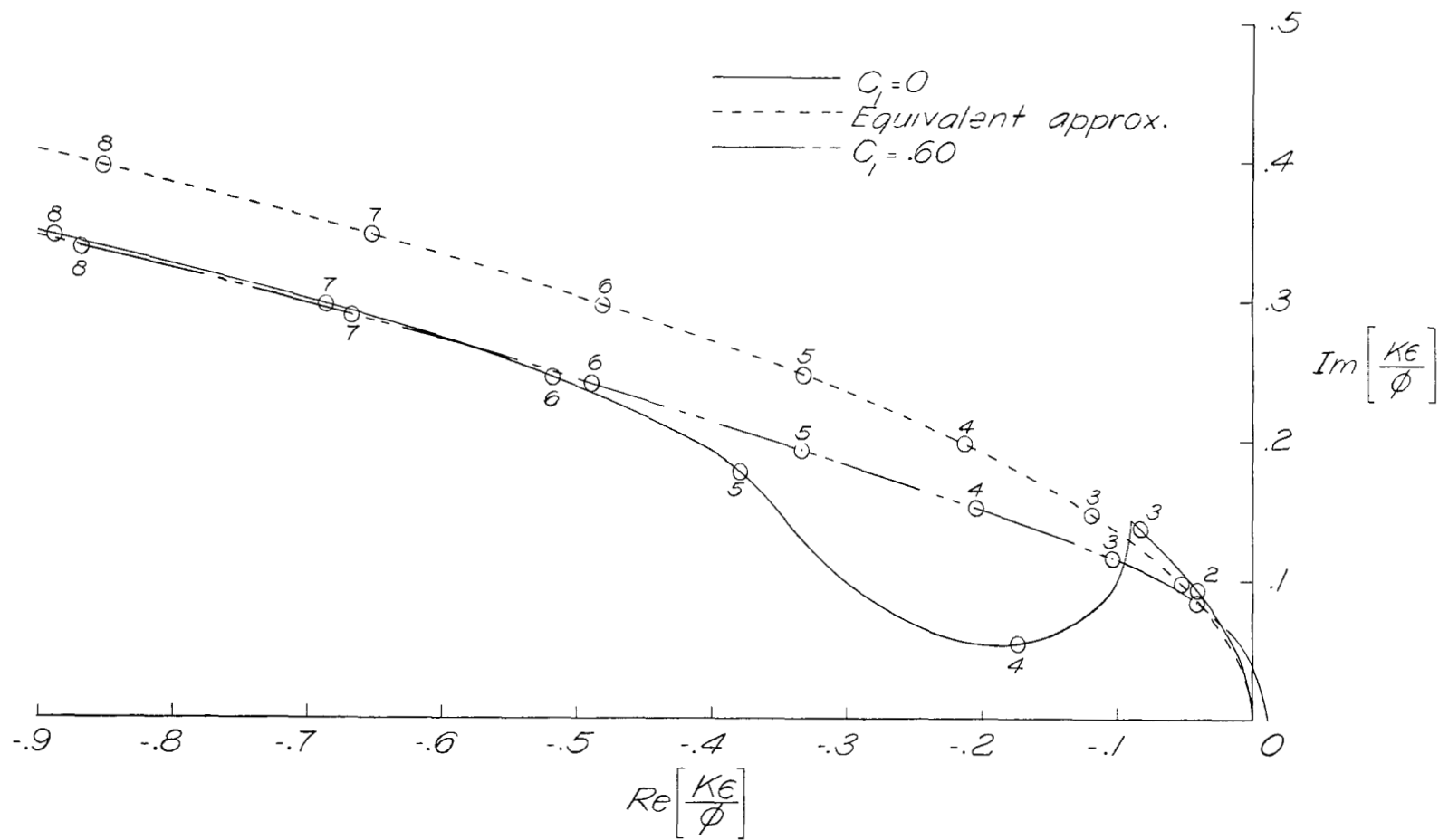


Figure 4.- Inverse open-loop complex plots for the four airplane configurations. Numbered points on all complex plots indicate values of  $\omega$  at each point.



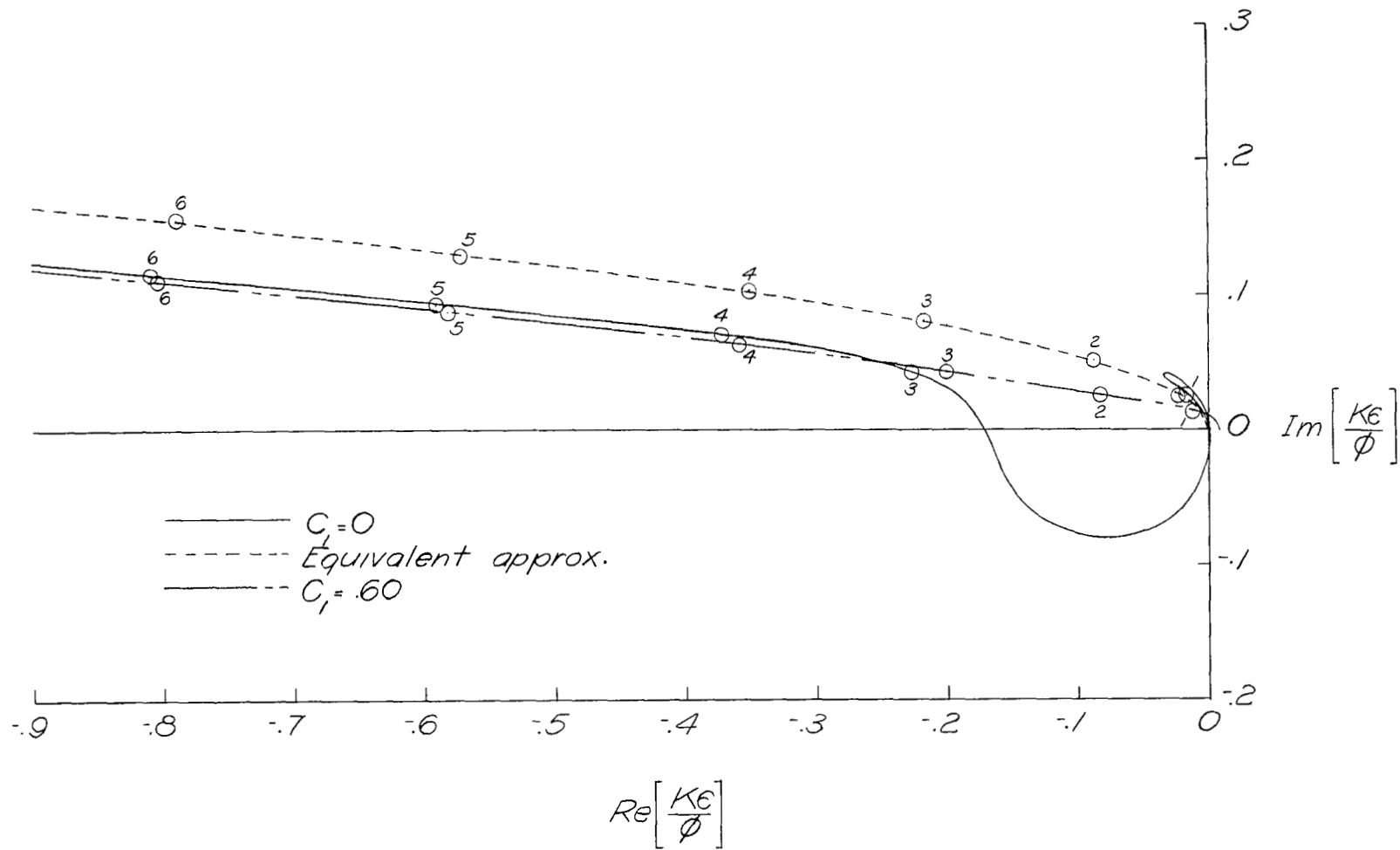
(a) Case A.

Figure 5.- Comparison of inverse open-loop complex plots for each airplane configuration alone, airplane with yaw damper, and equivalent approximation.



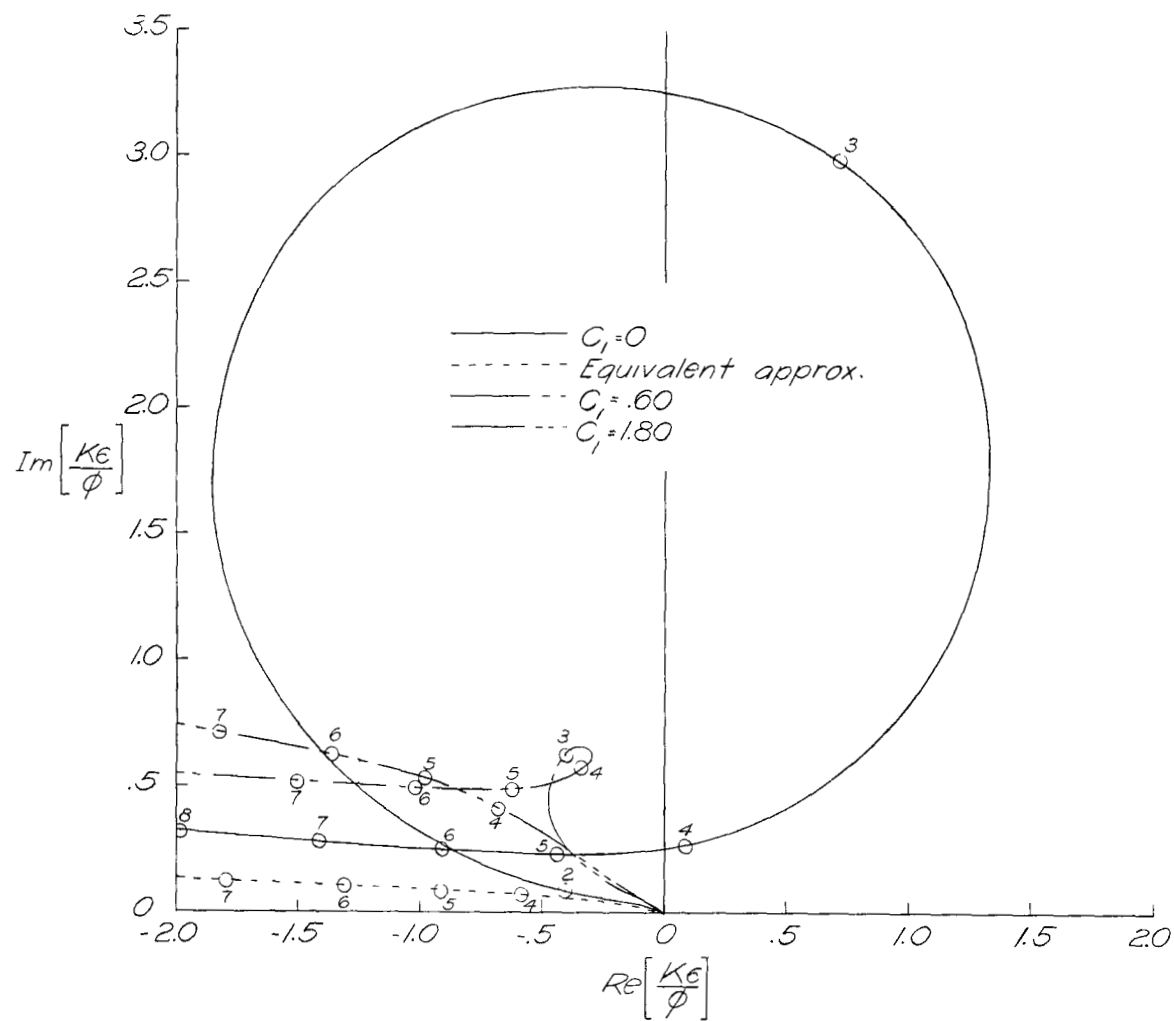
(b) Case B.

Figure 5.- Continued.



(c) Case C.

Figure 5.- Continued.



(d) Case D.

Figure 5.- Concluded.

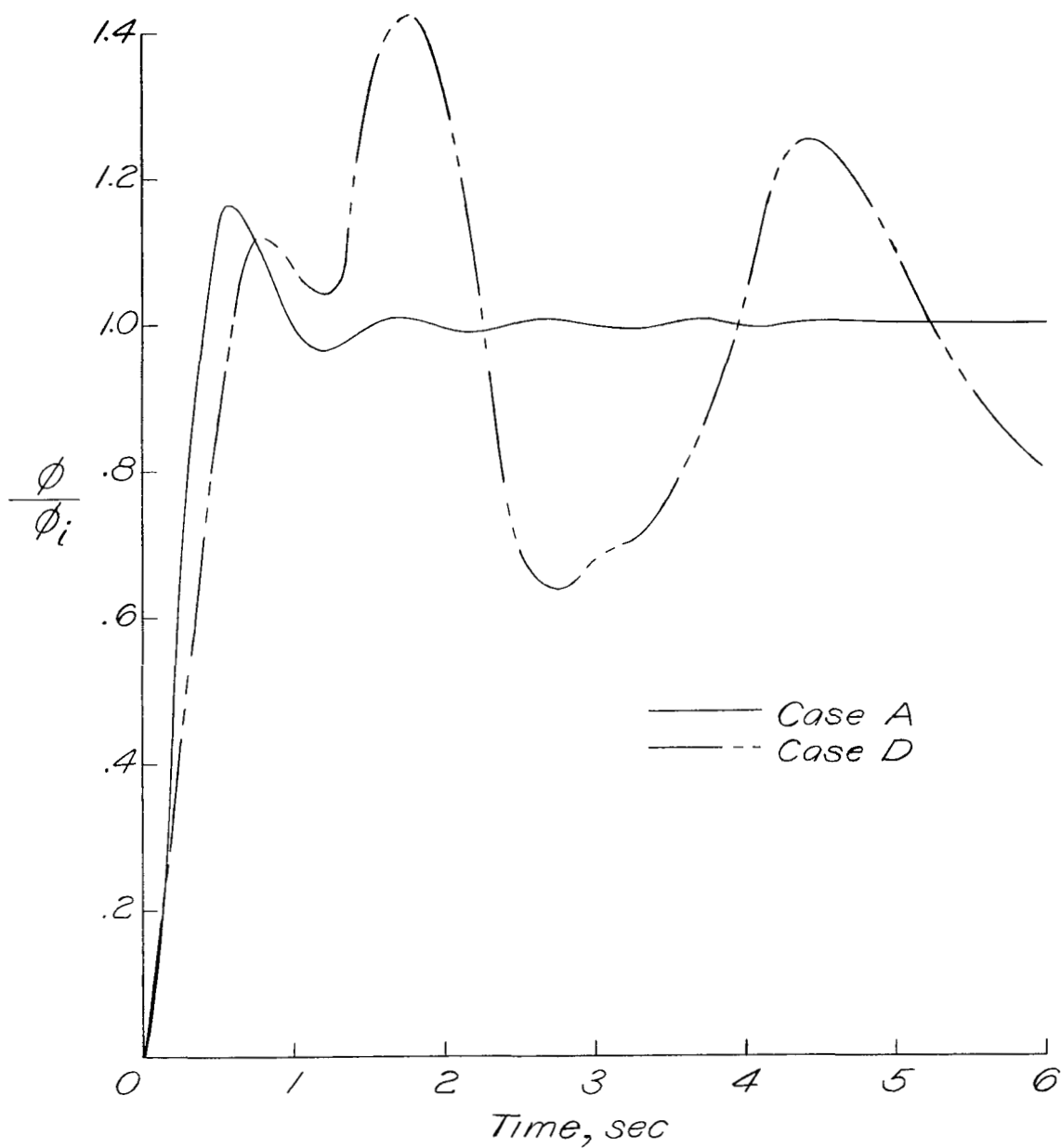


Figure 6.- Comparison of command responses of cases A and D with the simplest control system.  $K = 0.5$ .

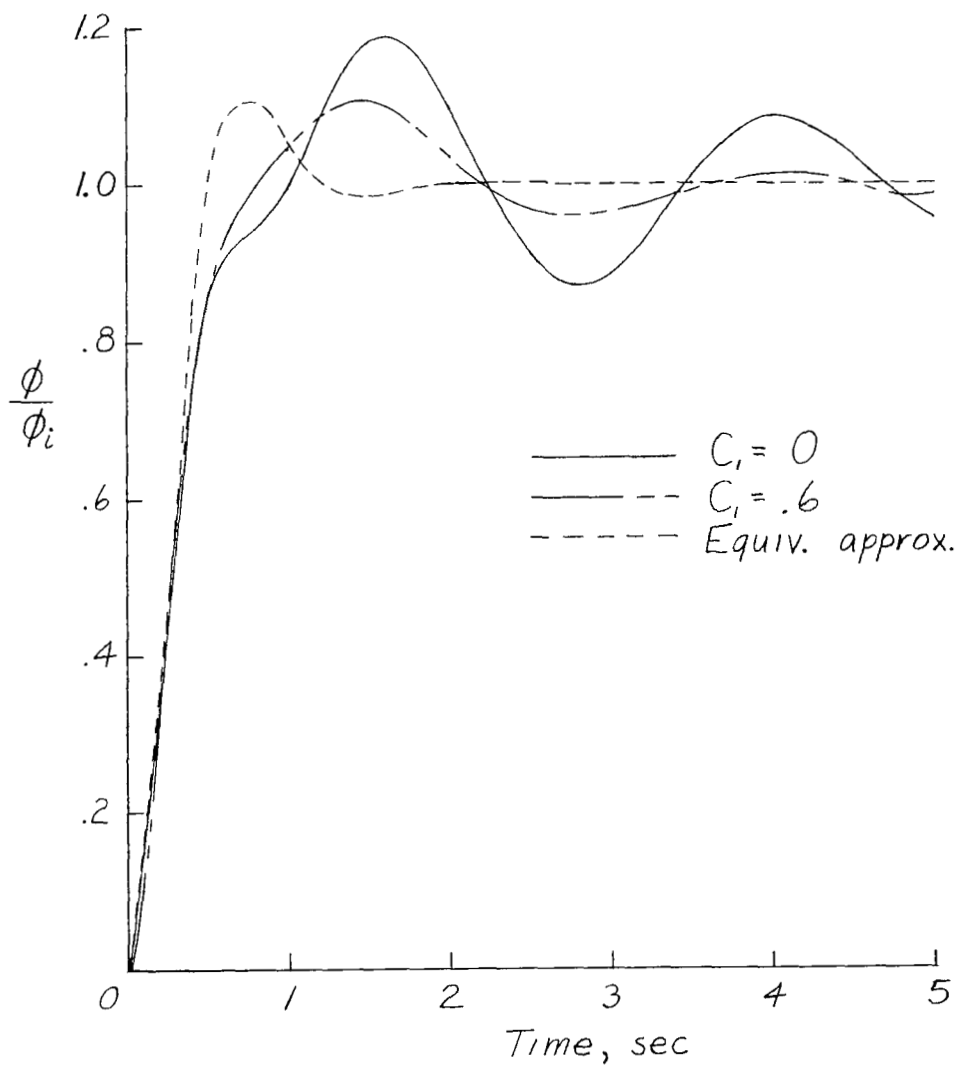


Figure 7.- Transients showing relative lack of effectiveness of yaw damper in eliminating Dutch-roll oscillation for airplane with large  $K_{XZ}$ . Case D with increased roll damping and  $K = 1$ .

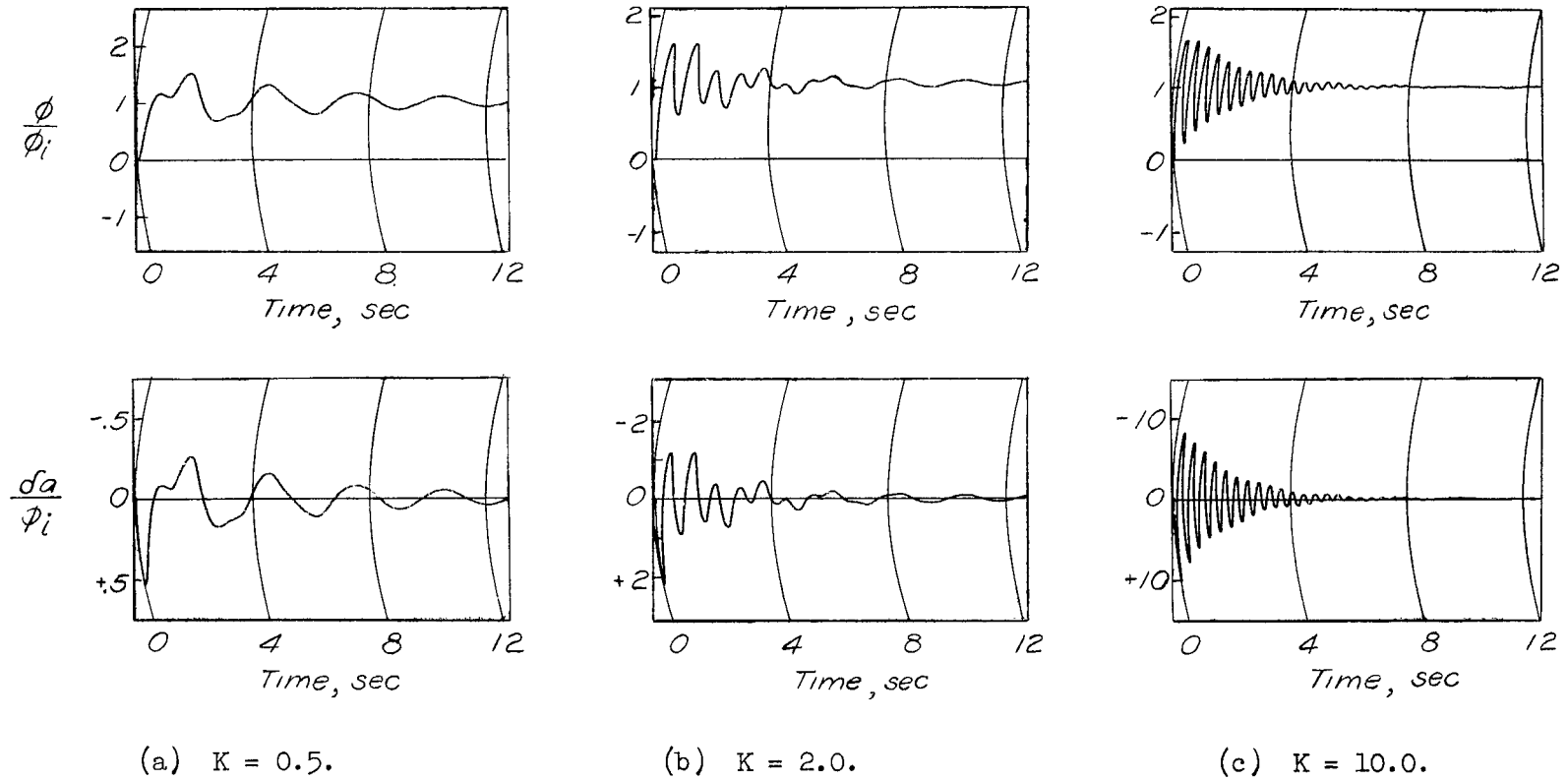


Figure 8.- Decrease of Dutch-roll effect for high gains. Command responses for case D.

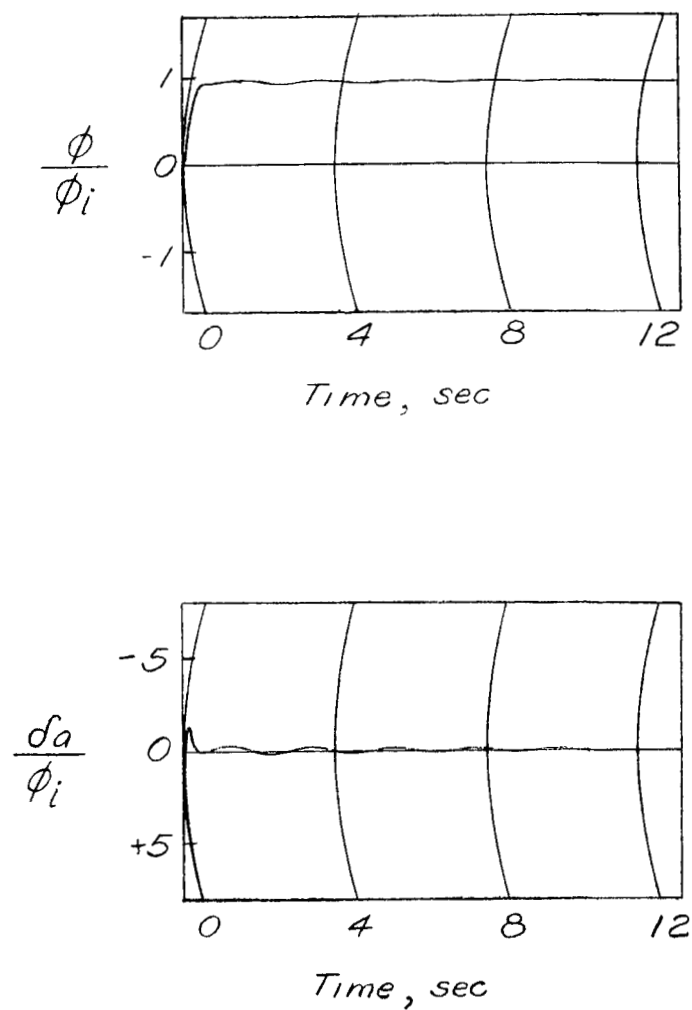
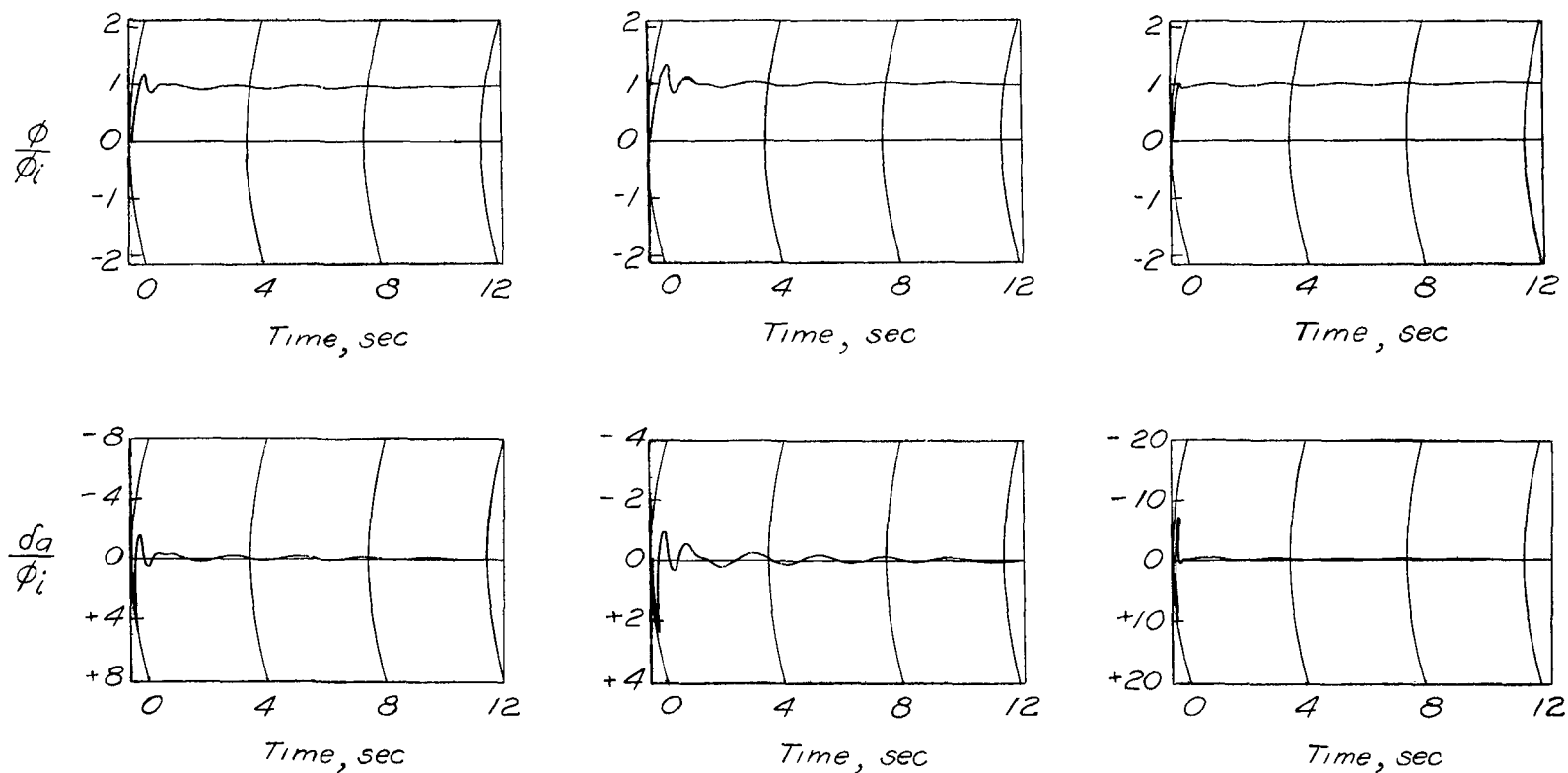


Figure 9.- Command response of case D for  $K = 10$  and  $K' = 0.5$ .

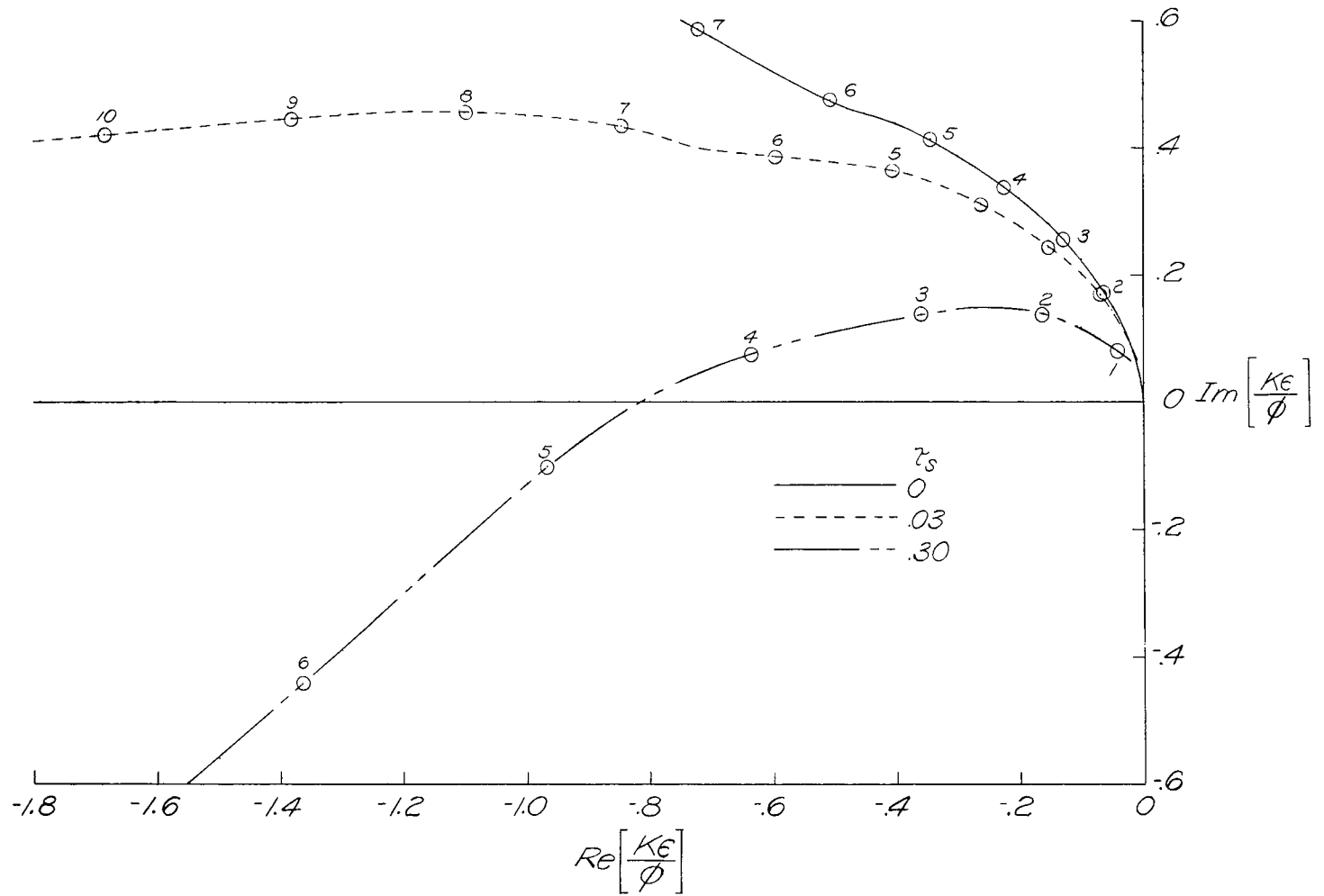


(a)  $K'' = 0$ .

(b)  $K'' = 0.035$ .

(c)  $K'' = -0.035$ .

Figure 10.- Effect of  $K''$  on command response of case D with  $K = 5$  and  $K' = 0.26$ .



(a) Case A.

Figure 11.- Effect of servo time lag on inverse open-loop complex plots.

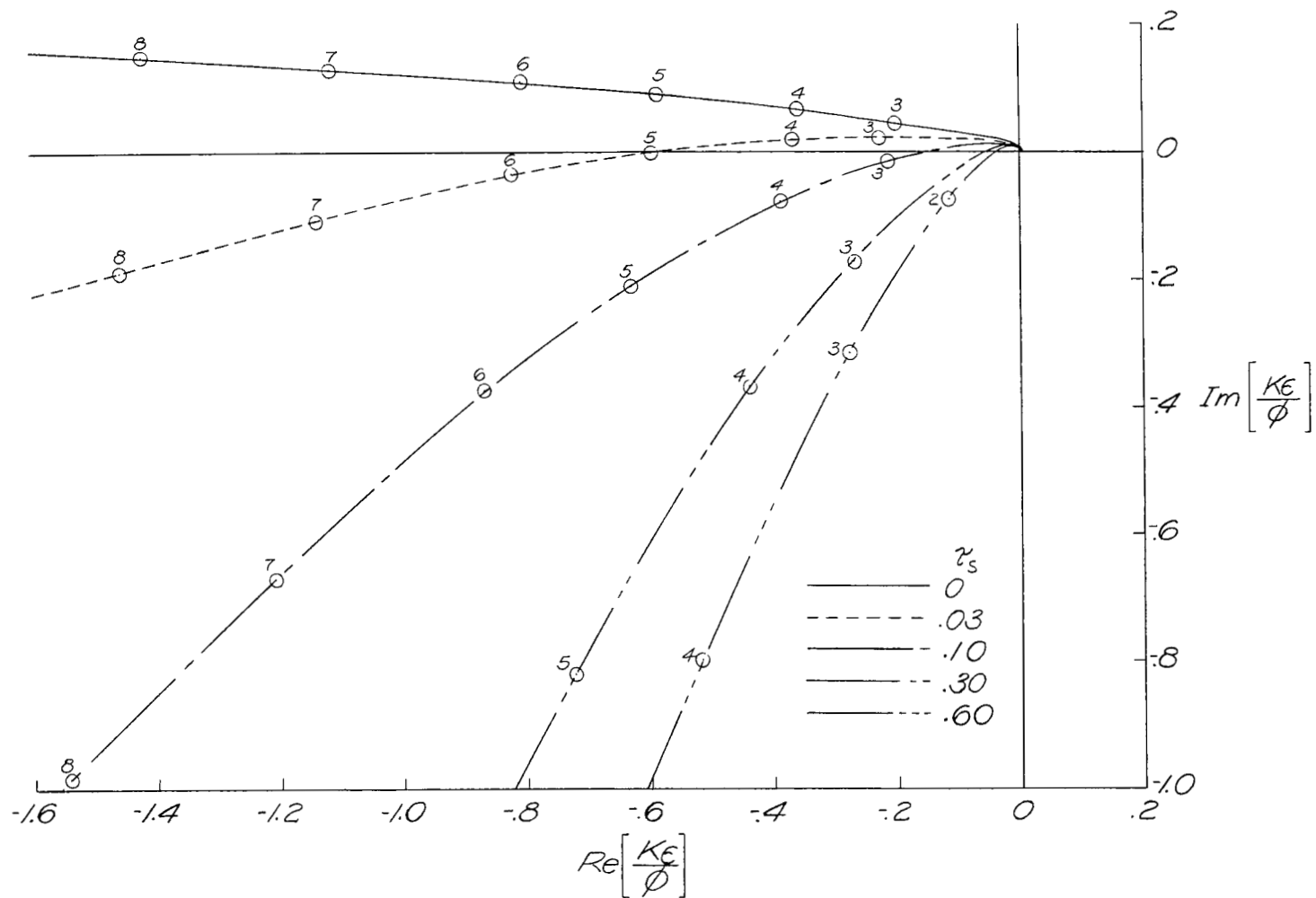
(b) Case C with  $C_1 = 0.6$ .

Figure 11.- Concluded.

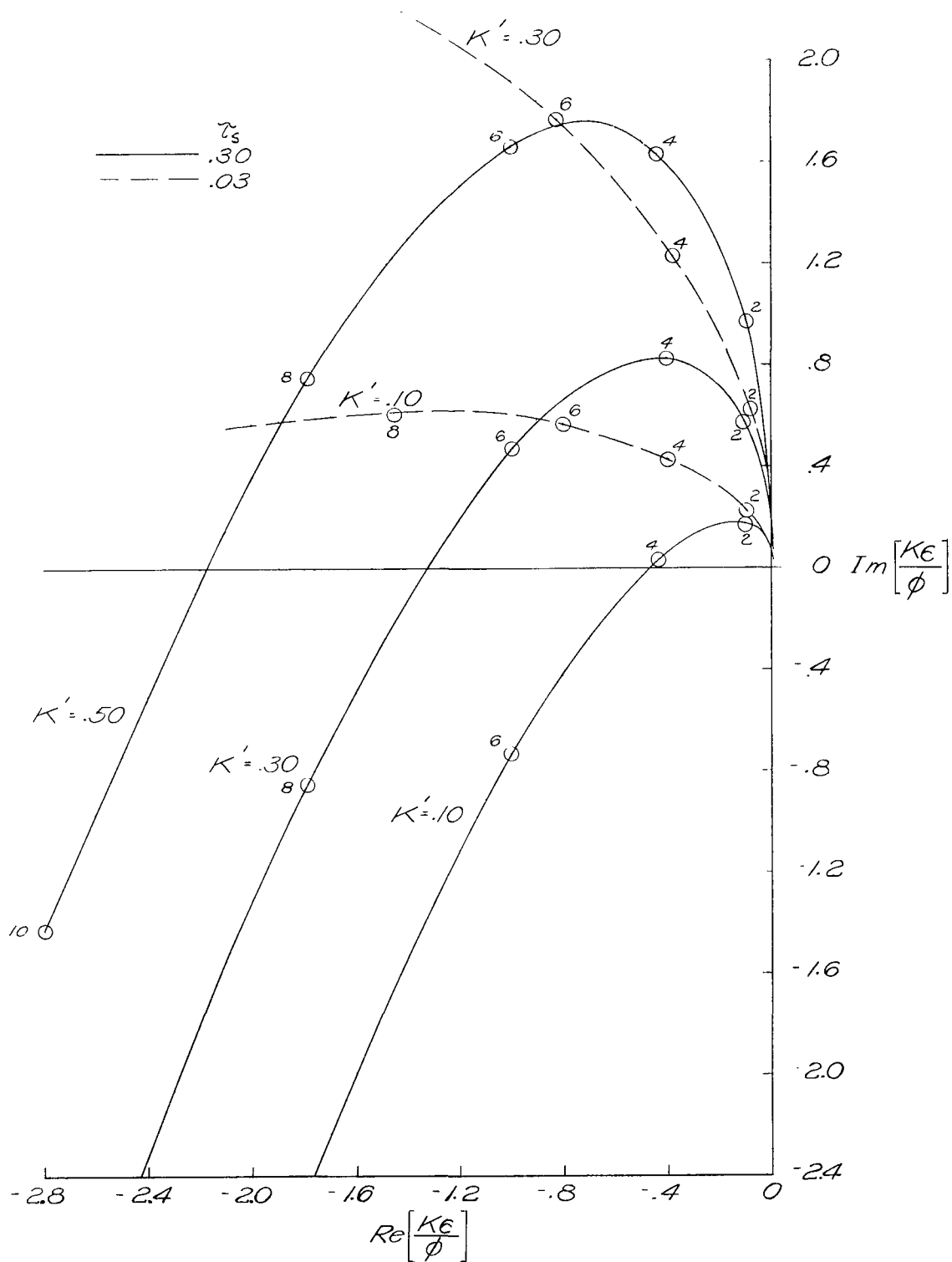


Figure 12.- Correction of time-lag destabilization by rate feedback.  
Inverse open loops for case C with  $C_1 = 0.6$ .

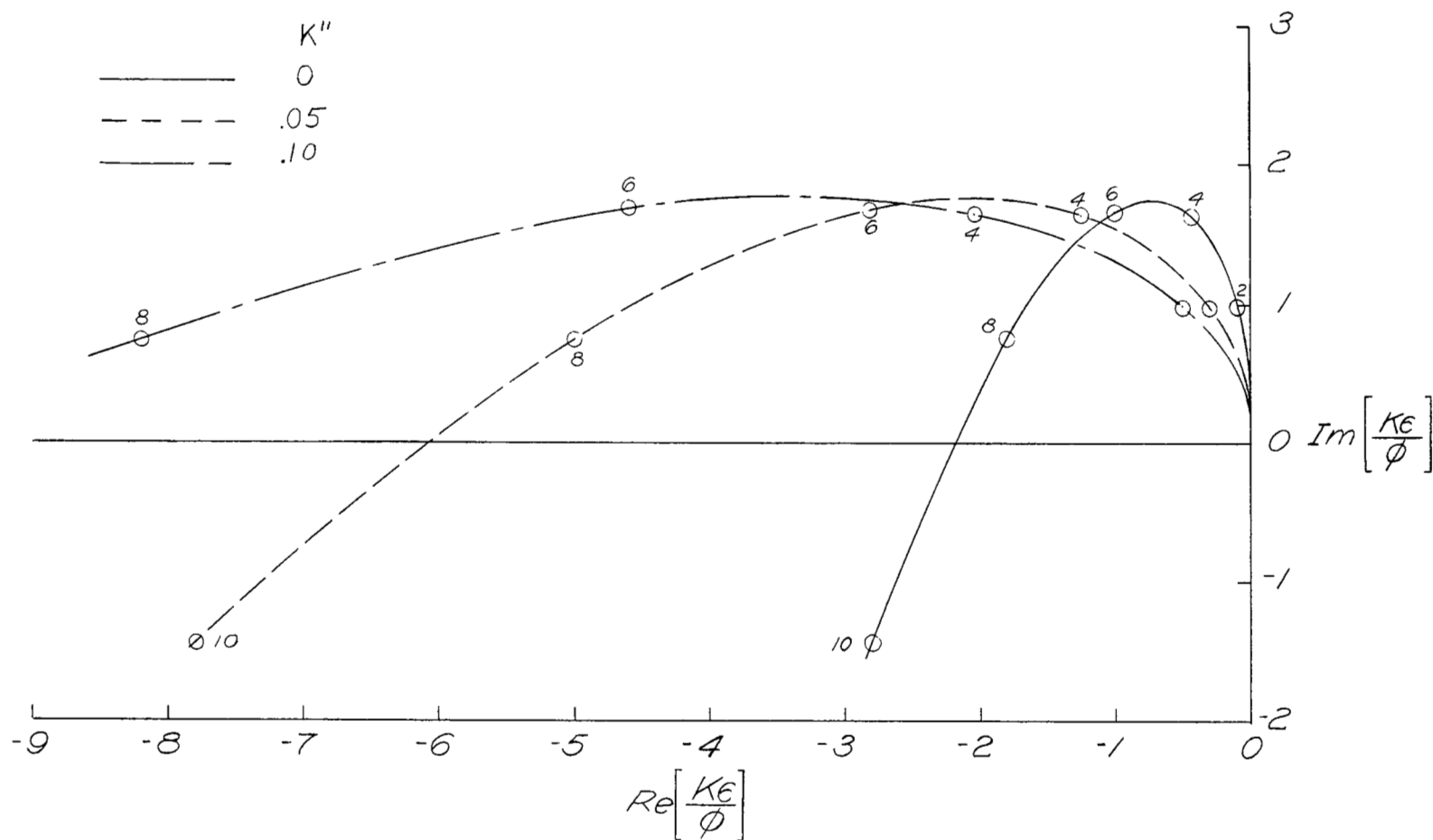


Figure 13.- Correction of time-lag destabilization by combined rate and acceleration feedbacks. Inverse open loops for case C with  $C_1 = 0.6$ ,  $K' = 0.5$ , and  $\tau_s = 0.3$ .

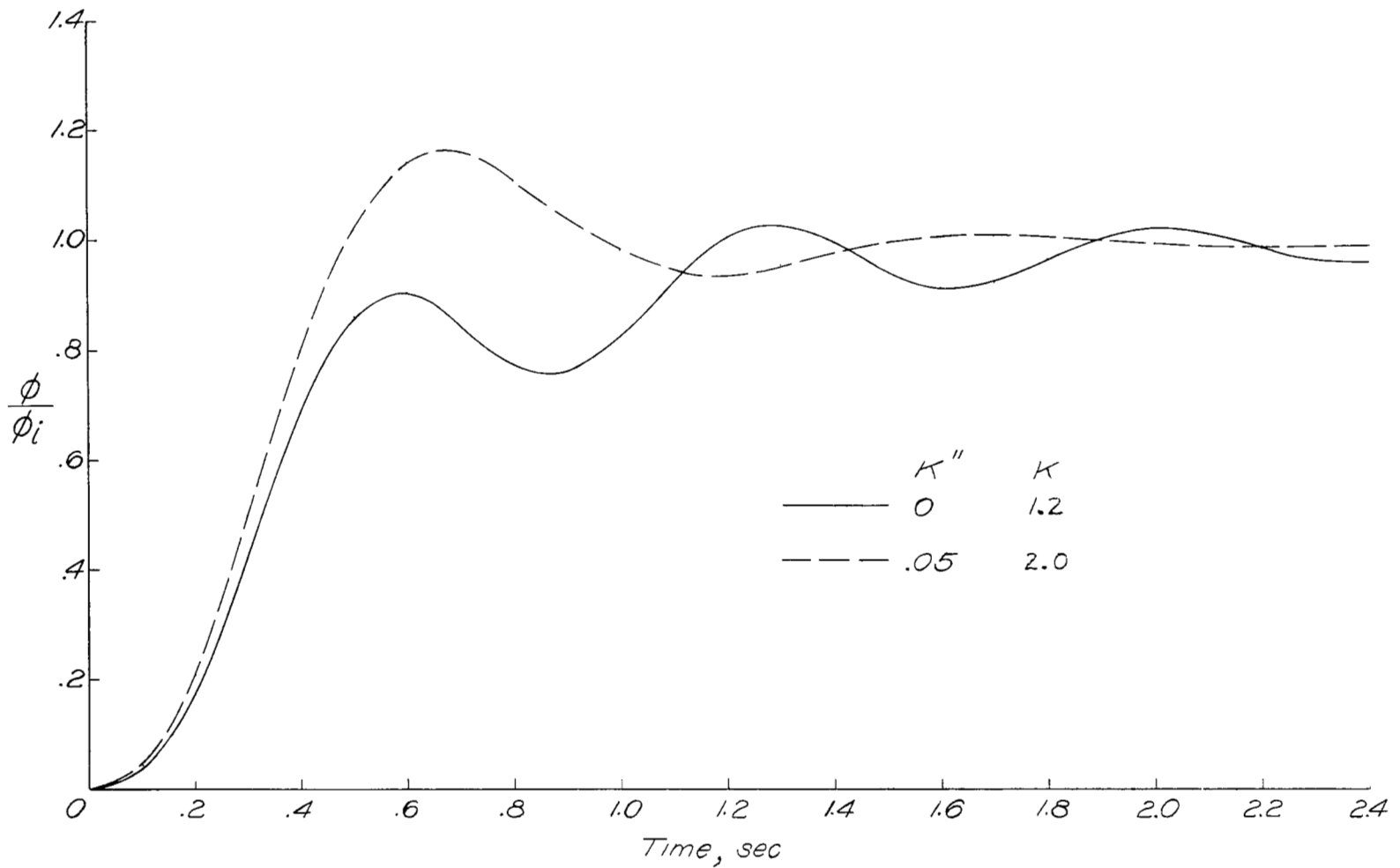


Figure 14.- Effect of acceleration feedback on command-response transient at optimum gain. Case C with  $C_1 = 0.6$ ,  $K' = 0.5$ , and  $\tau_s = 0.3$ .

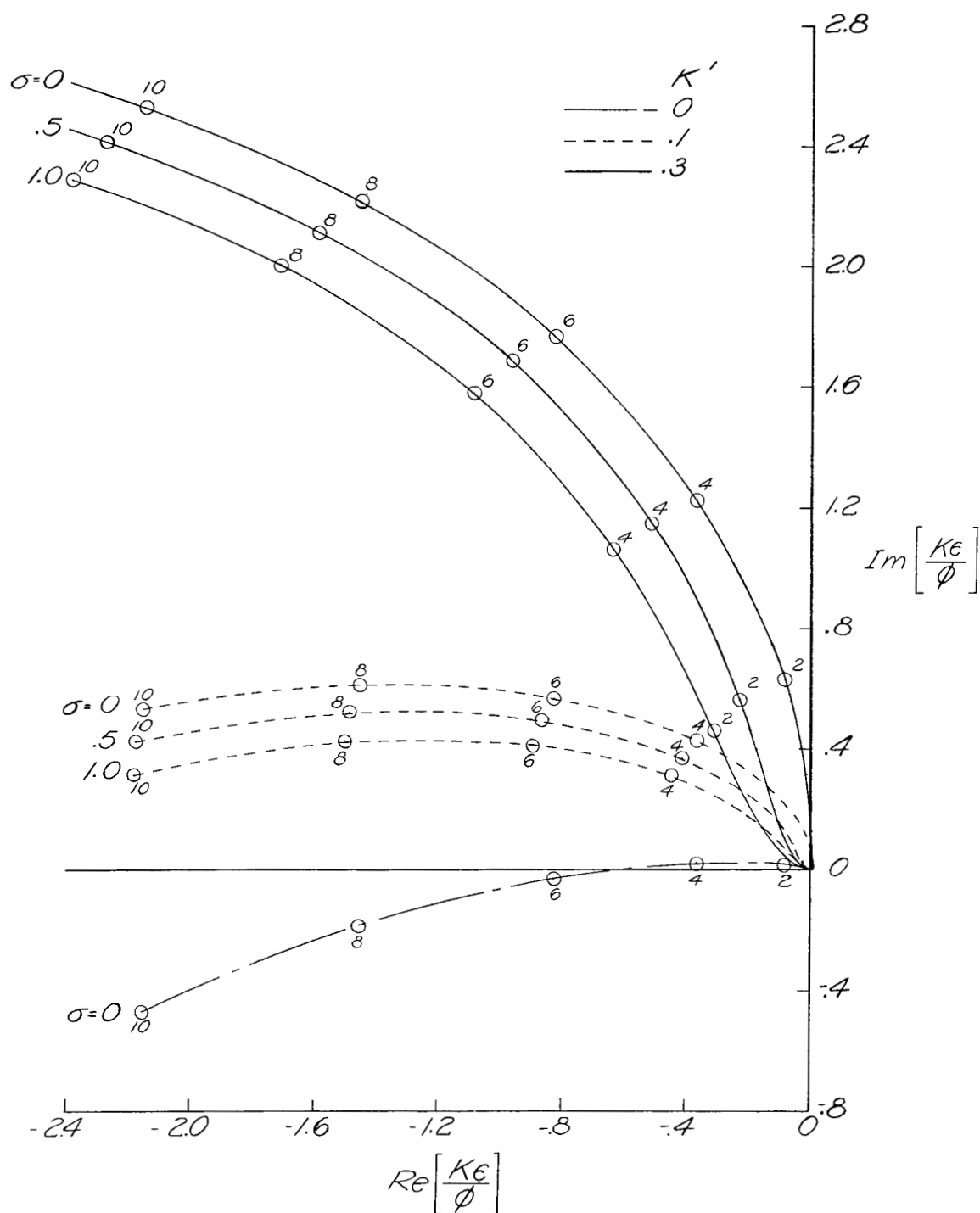


Figure 15.- Effect of integrator ratio  $\sigma$  on inverse open-loop responses for different amounts of rate feedback. Case C with  $\tau_s = 0.03$  and  $C_1 = 0.6$ .

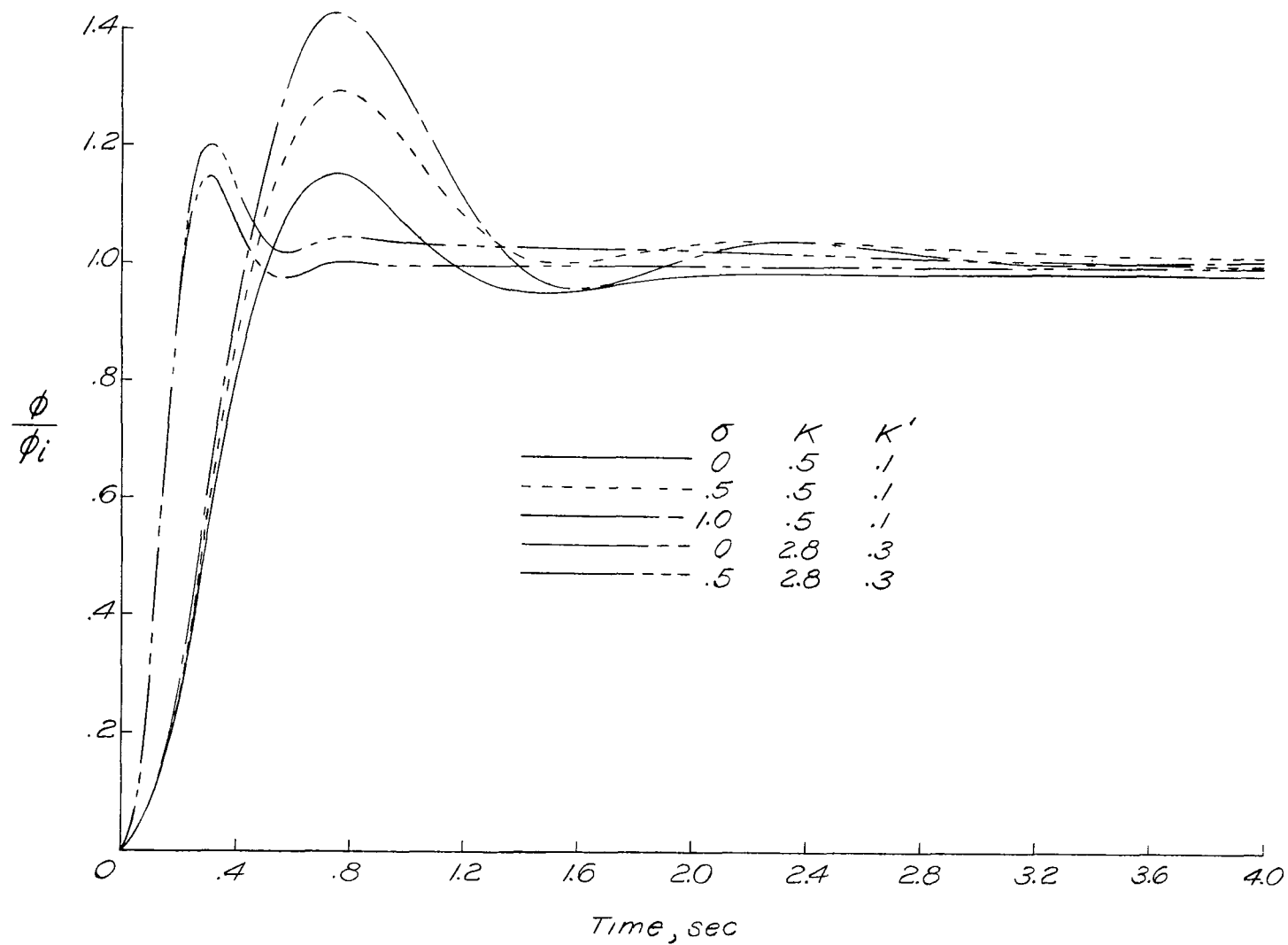


Figure 16.- Transients showing the decrease of integrator overshoot for higher sensitivity gain. Case C with  $\tau_s = 0.03$  and  $C_1 = 0.6$ .

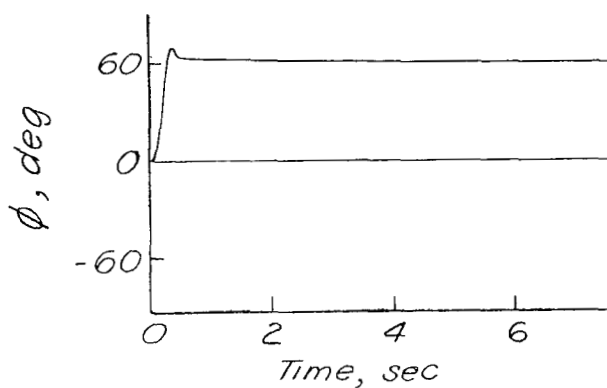
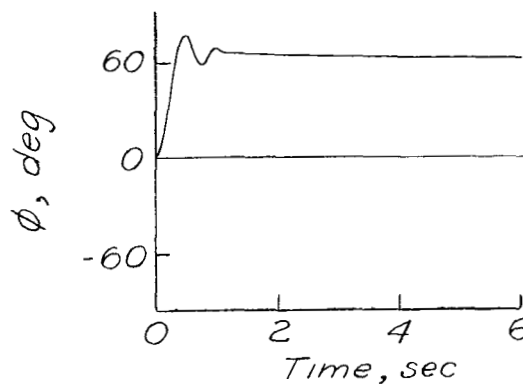
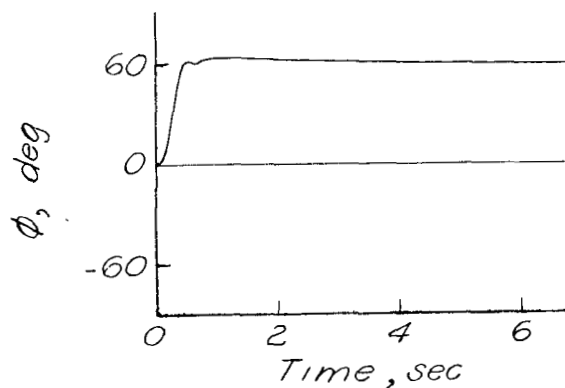
(a)  $K' = 0.4$ ; high limits.(b)  $K' = 0.4$ ;  $\delta_{aL} = 20^\circ$ ;  $\dot{\delta}_{aL} = 120^\circ \text{ sec}^{-1}$ .(c)  $K' = 0.6$ ;  $\delta_{aL} = 20^\circ$ ;  $\dot{\delta}_{aL} = 120^\circ \text{ sec}^{-1}$ .

Figure 17.- Transients showing that even high rate limits may introduce oscillations and that rate-feedback may be helpful. Case A with  $K = 3$ ,  $K_I = 1$ , and  $C_I = 0.3$ .

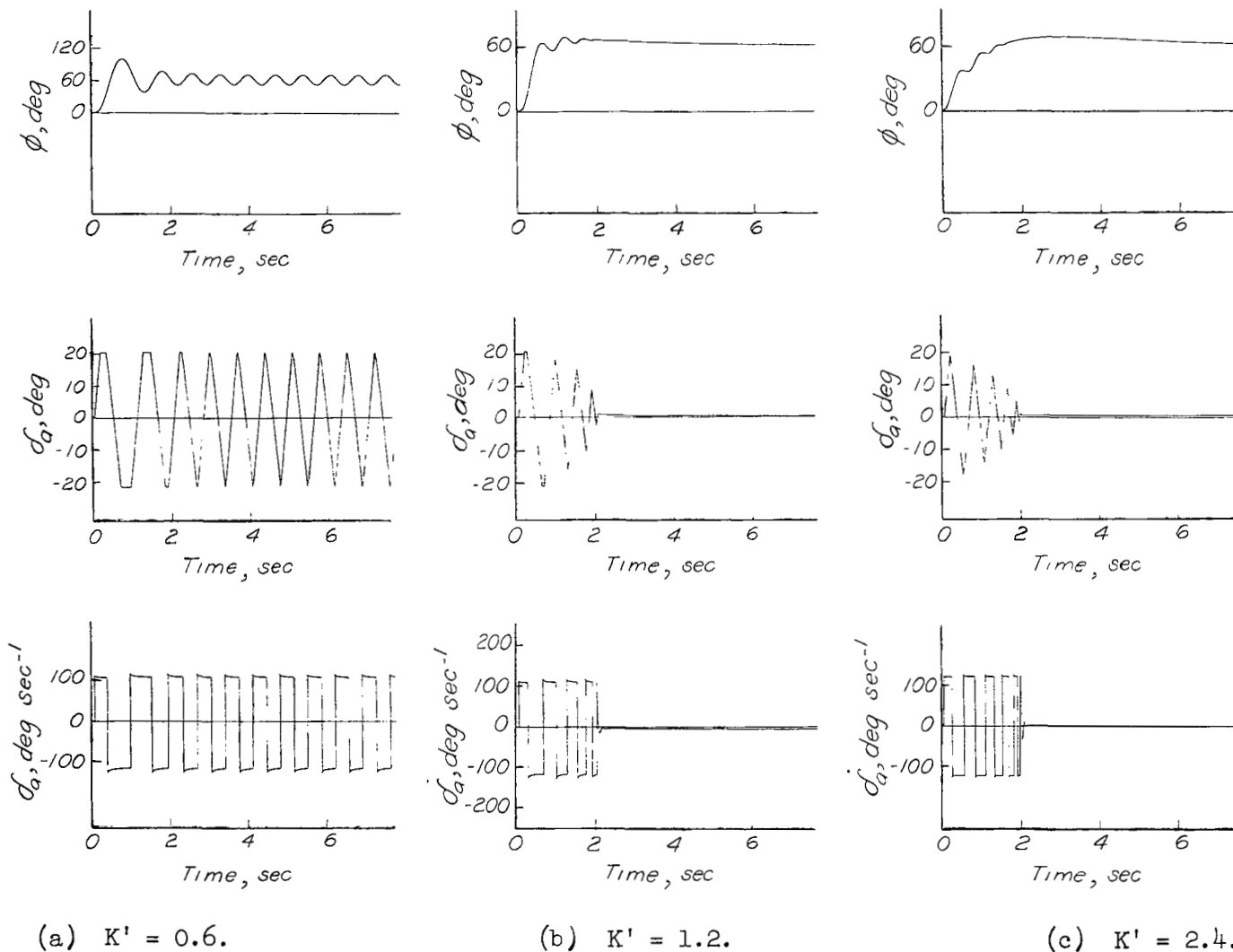
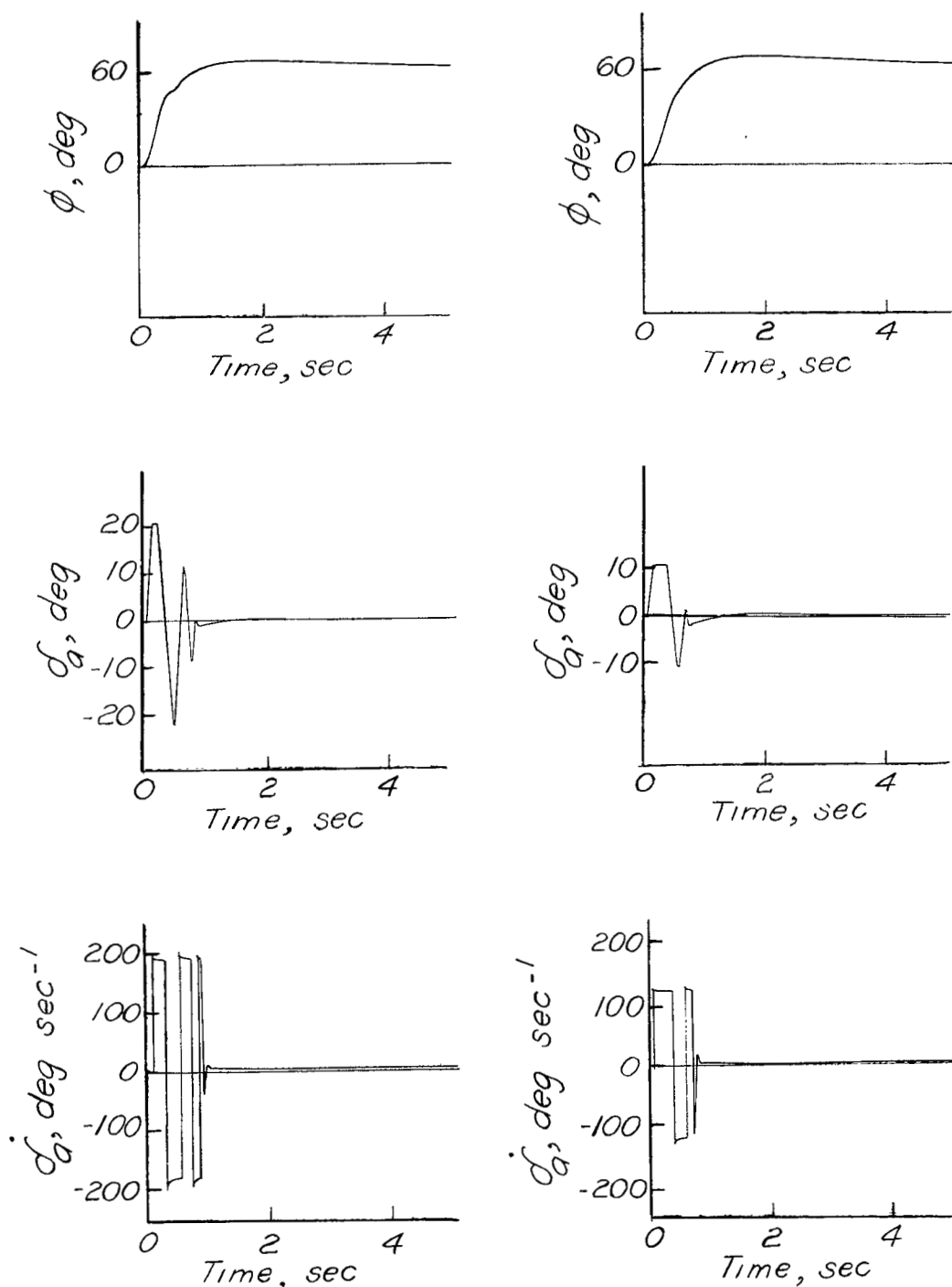
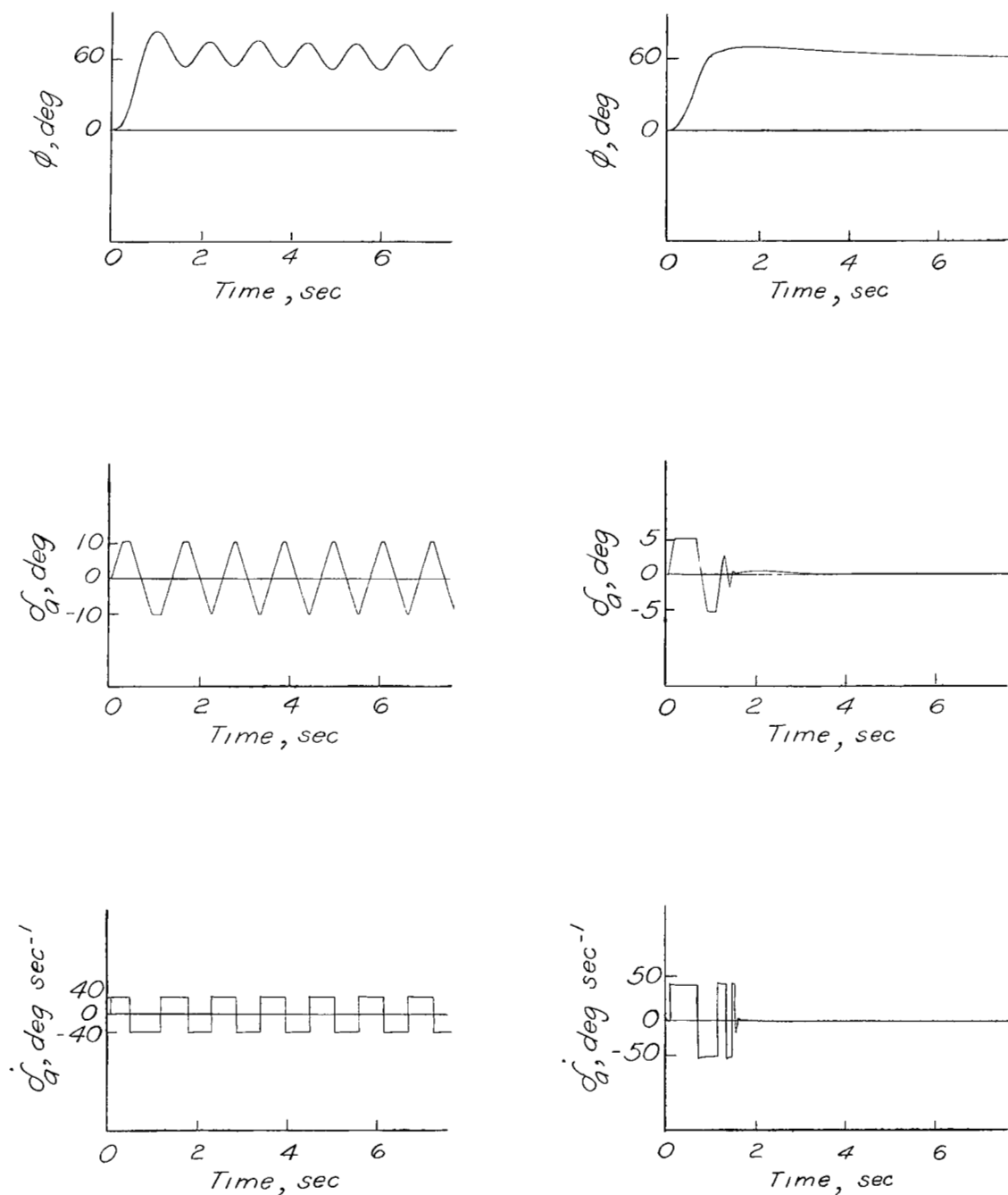


Figure 18.- Ineffectiveness of rate feedback for eliminating the rate-limiting oscillation in Case C.  $K = 3$ ,  $K_I = 1$ , and  $C_I = 0.3$ .



(a)  $\delta_{aL} = 20^\circ$ ;  $\dot{\delta}_{aL} = 180^\circ \text{ sec}^{-1}$ .      (b)  $\delta_{aL} = 10^\circ$ ;  $\dot{\delta}_{aL} = 120^\circ \text{ sec}^{-1}$ .

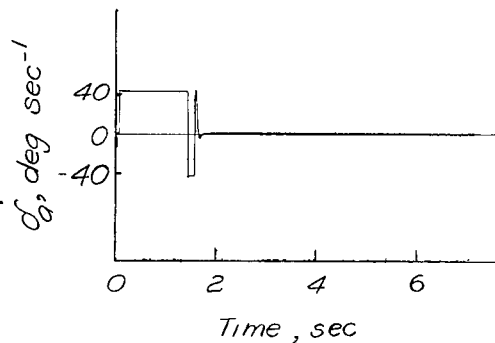
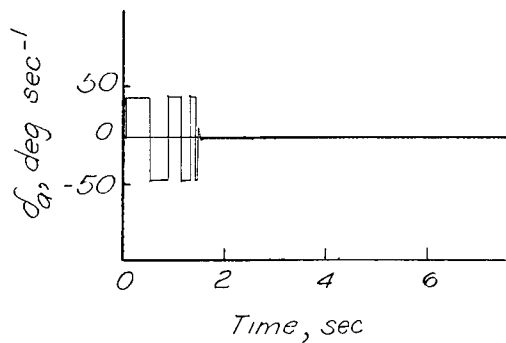
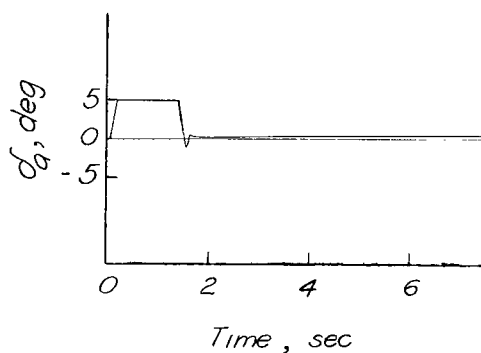
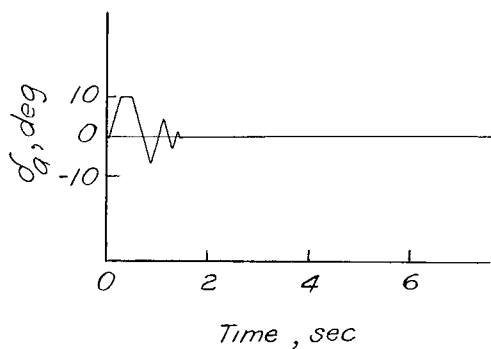
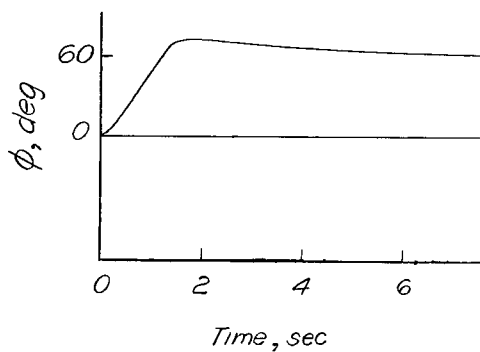
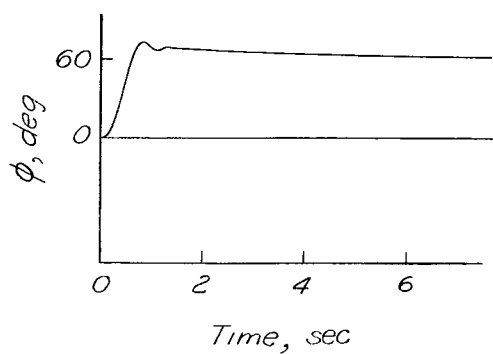
Figure 19.- Effects of increased rate limits and of decreased deflection limits on the limiting oscillation. (Compare with fig. 18(b).)



(a)  $\delta_{aL} = 10^\circ$ ;  $\dot{\delta}_{aL} = 40^\circ \text{ sec}^{-1}$ .

(b)  $\delta_{aL} = 5^\circ$ ;  $\dot{\delta}_{aL} = 40^\circ \text{ sec}^{-1}$ .

Figure 20.- Effect of lower value of control-rate limit for case C.  
(Compare with fig. 19.)



(a)  $\delta_{aL} = 10^\circ$ ;  $\dot{\delta}_{aL} = 40^\circ \text{ sec}^{-1}$ .      (b)  $\delta_{aL} = 5^\circ$ ;  $\dot{\delta}_{aL} = 40^\circ \text{ sec}^{-1}$ .

Figure 21.- Illustration of increased rise time generally resulting from low deflection limit. Case A (same autopilot as for case C).

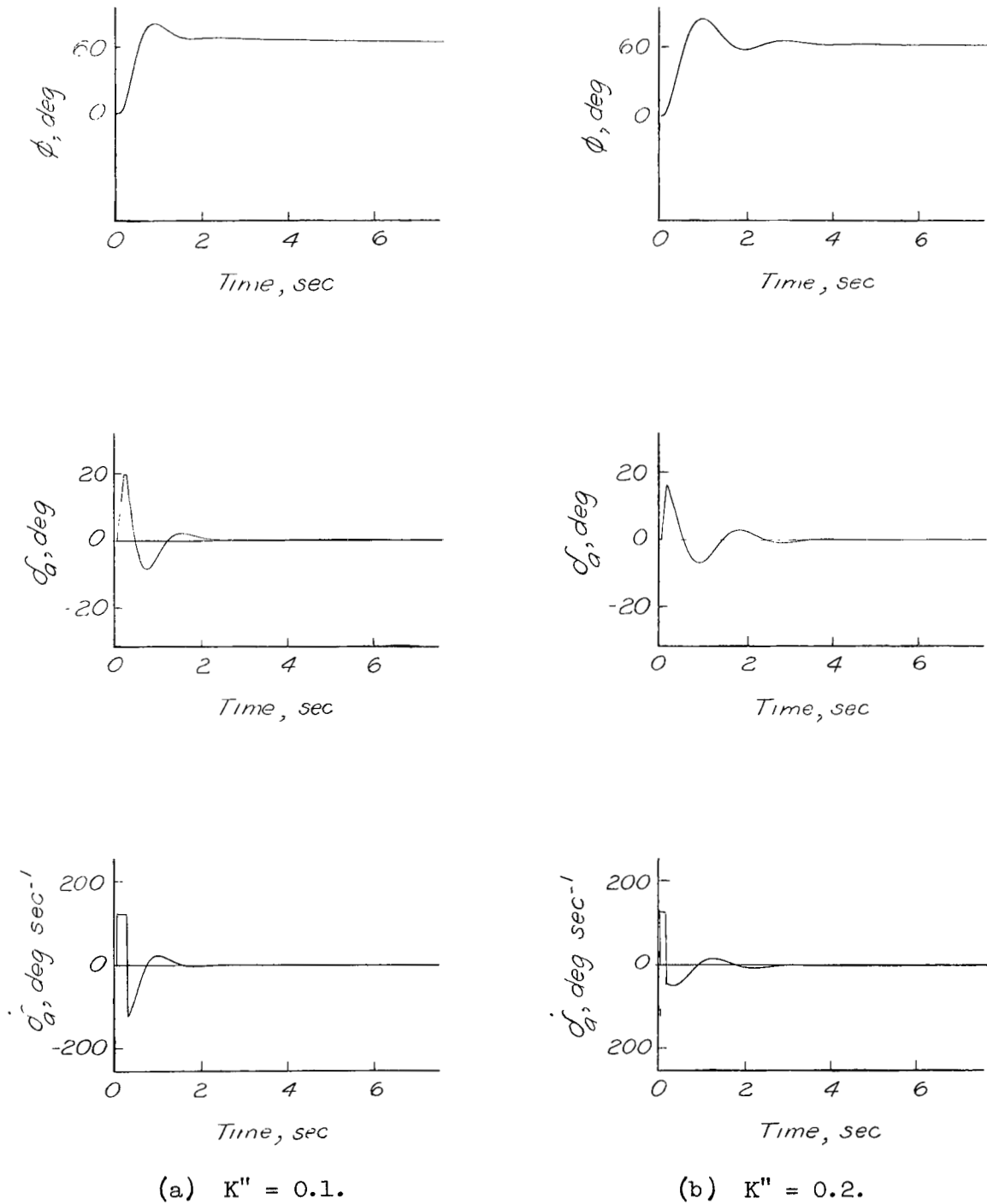


Figure 22.- Response of neutrally stable system of figure 18(a) with added acceleration feedback.

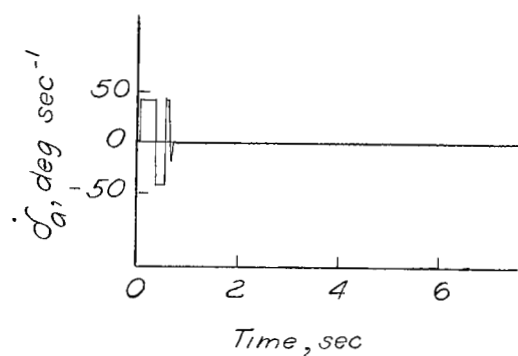
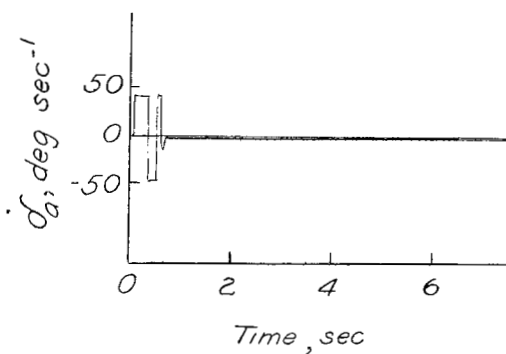
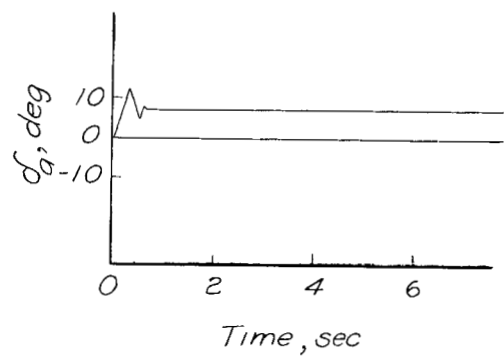
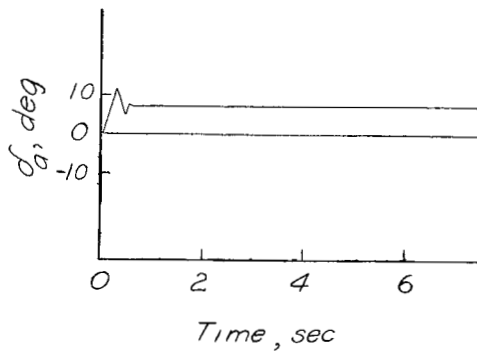
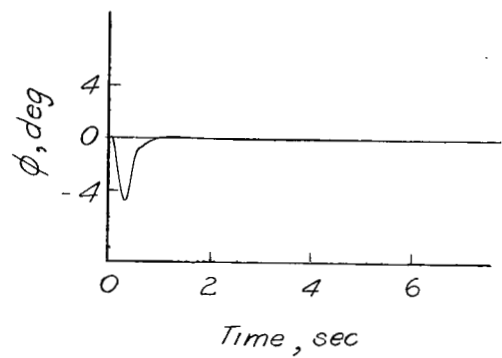
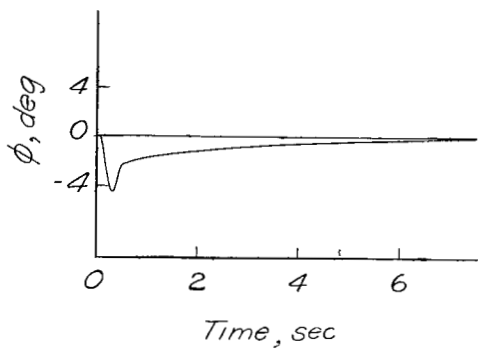
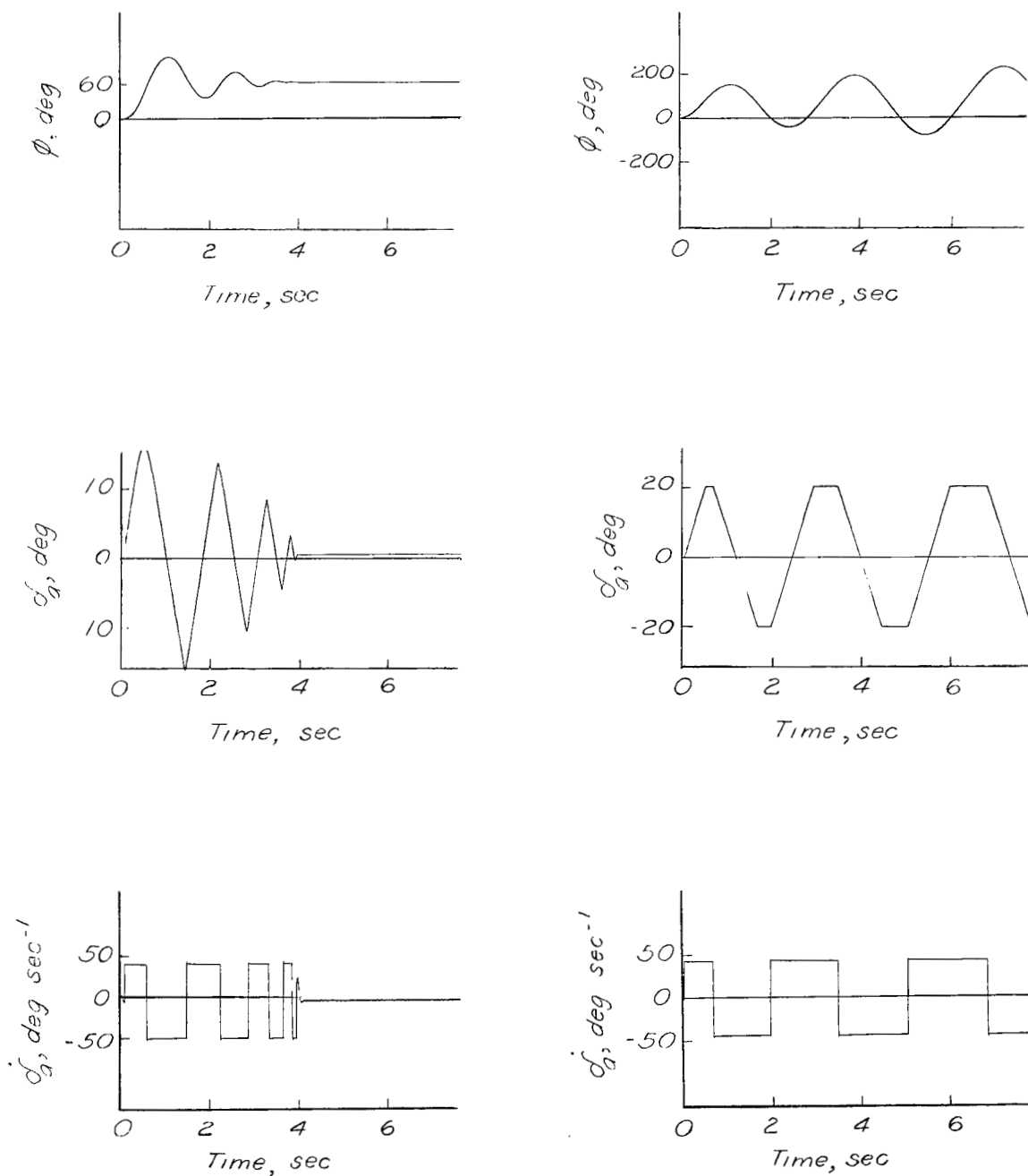
(a)  $K_I = 1.0$ .(b)  $K_I = 5.0$ .

Figure 23.- Effect of integral gain on regulatory response with limiting. Case A with  $K = 3$ ,  $K' = 0.6$ ,  $C_1 = 0.3$ ,  $\delta_{aL} = 20^\circ$ , and  $\dot{\delta}_{aL} = 40^\circ \text{ sec}^{-1}$ ; steady disturbance;  $\delta_{a0} = 8^\circ$ .



(a)  $K_I = 1.0$ ;  $\delta_{aL} = 20^\circ$ ;  
 $\dot{\delta}_{aL} = 40^\circ \text{ sec}^{-1}$ .

(b)  $K_I = 5.0$ ;  $\delta_{aL} = 20^\circ$ ;  
 $\dot{\delta}_{aL} = 40^\circ \text{ sec}^{-1}$ .

Figure 24.- Destabilization of limiting oscillation by integral gain.  
 Command responses for systems shown in figure 23.

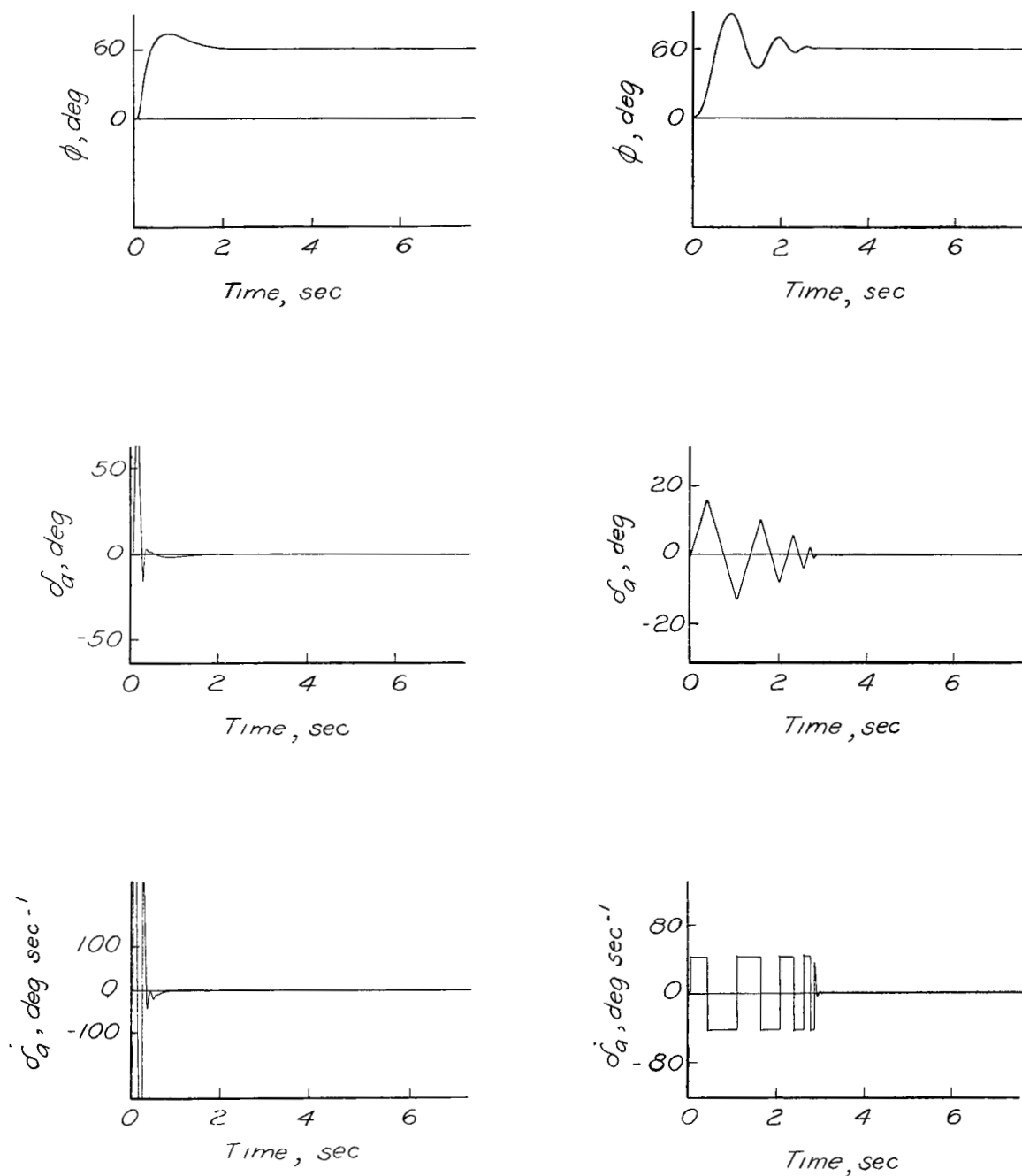
(a)  $K_I = 5.0$ ; high limits.(b)  $K_I = 0$ ;  $\delta_{aL} = 20^\circ$ ;  
 $\dot{\delta}_{aL} = 40^\circ \text{ sec}^{-1}$ .

Figure 25.- Command responses for systems of figure 24(b) with high limits and figure 24(a) without integral.

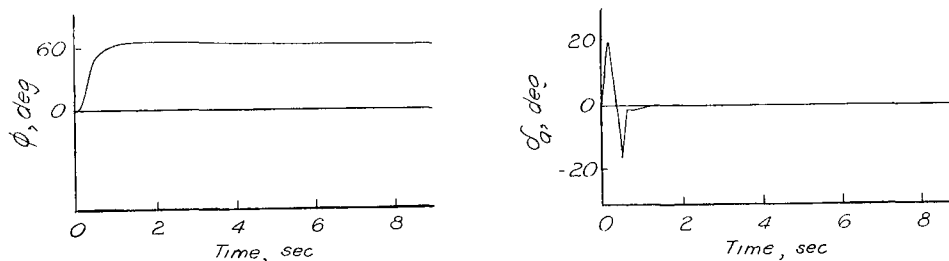
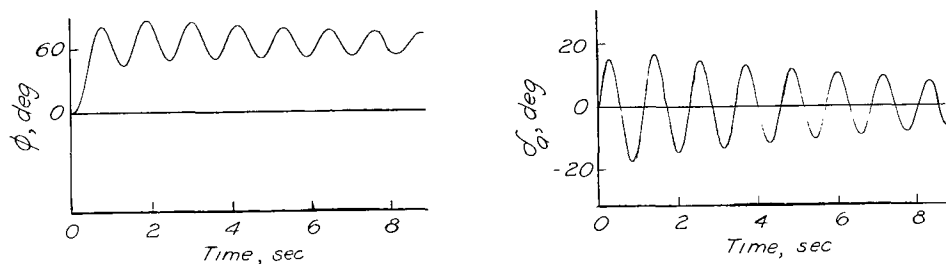
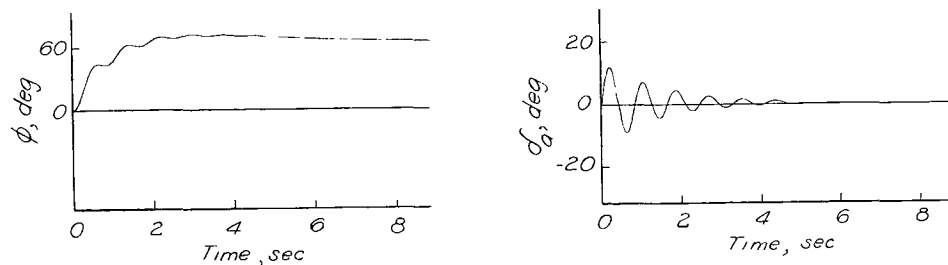
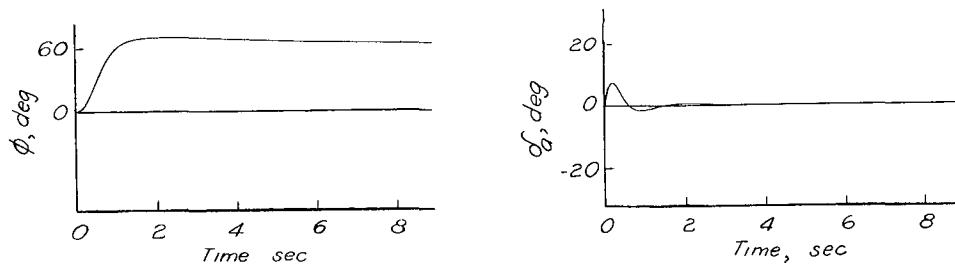
(a)  $\tau_s = 0.015$  sec;  $K' = 0.4$ ;  $K'' = 0$ .(b)  $\tau_s = 0.3$  sec;  $K' = 0.4$ ;  $K'' = 0$ .(c)  $\tau_s = 0.3$  sec;  $K' = 0.8$ ;  $K'' = 0$ .(d)  $\tau_s = 0.3$  sec;  $K' = 0.6$ ;  $K'' = 0.1$ .

Figure 26.- Destabilizing effect of increased time lag, and improvement through use of rate and acceleration feedbacks. Case C with  $K = 1$ ,  $K_I = 0.25$ , and  $C_1 = 0.3$ .

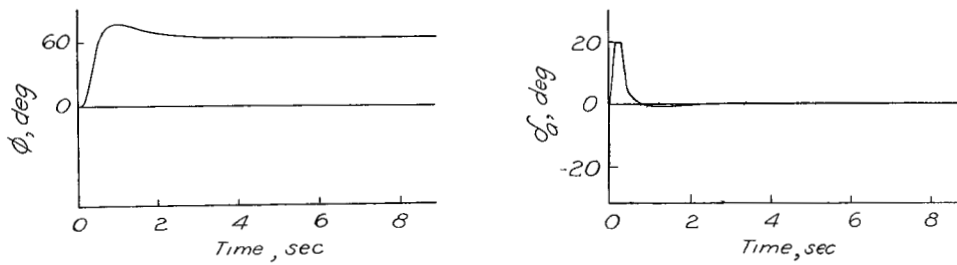
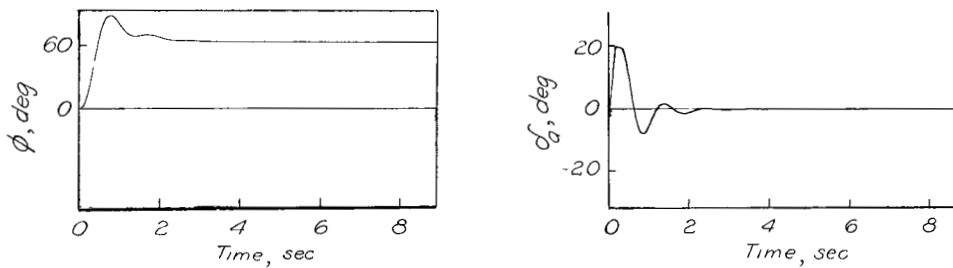
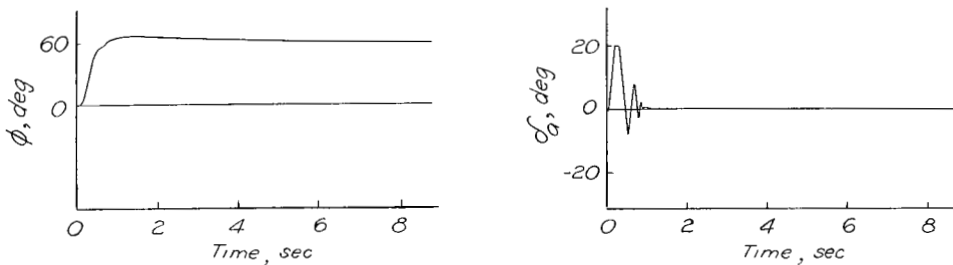
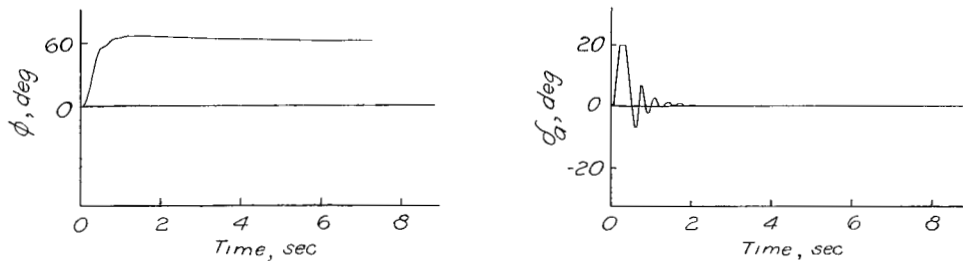
(a)  $\tau_s = 0.015$  sec;  $K = 1$ ;  $K' = 0.2$ .(b)  $\tau_s = 0.3$  sec;  $K = 1$ ;  $K' = 0.2$ .(c)  $\tau_s = 0.015$  sec;  $K = 6$ ;  $K' = 1.6$ .(d)  $\tau_s = 0.3$  sec;  $K = 6$ ;  $K' = 1.6$ .

Figure 27.- Comparison of time-lag effect for lower and higher gain combinations. Case A with  $C_L = 0.3$ ,  $\delta_{aL} = 20^\circ$ , and  $\delta_{aL} = 120^\circ \text{ sec}^{-1}$ .

LANGLEY RESEARCH CENTER



3 1176 00507 5412